International Journal of Heat and Mass Transfer 137 (2019) 1263–1289

Contents lists available at ScienceDirect

International Journal of Heat and Mass Transfer

journal homepage: www.elsevier.com/locate/ijhmt

Review

A review of current progress in multiscale simulations for fluid flow and heat transfer problems: The frameworks, coupling techniques and future perspectives

Zi-Xiang Tong [a], Ya-Ling He [b,*], Wen-Quan Tao [b]

[a] School of Human Settlements and Civil Engineering, Xi'an Jiaotong University, Xi'an 710049, PR China
[b] Key Laboratory of Thermo-Fluid Science and Engineering of Ministry of Education, School of Energy and Power Engineering, Xi'an Jiaotong University, No.28 Xianning West Road, Xi'an, Shaanxi 710049, PR China

ARTICLE INFO

Article history:
Received 3 October 2018
Received in revised form 14 March 2019
Accepted 1 April 2019

Keywords:
Multiscale simulation
Frameworks
Domain decomposition
Hierarchical
Multiple time scale
Flow and heat transfer

ABSTRACT

Many heat transfer and fluid flow problems are multiscale in nature, and the multiscale numerical methods are needed to solve the problems by considering the phenomena in all the scales. In this paper, the current progresses of the multiscale simulations for fluid flow and heat transfer problems are reviewed. Brief introductions of the numerical methods in different scales are given, which include macroscopic continuum methods, mesoscopic particle-based lattice Boltzmann, direct simulation Monte Carlo, dissipative particle dynamics and microscopic molecular dynamics. Then the classifications, frameworks and general procedures of the multiscale methods are proposed and discussed. The multiscale methods are divided into the domain decomposition scheme and hierarchical scheme. For the domain decomposition, the information exchange techniques among the numerical methods in different scales are surveyed. Special attentions are paid to the characteristics of the mesoscopic methods that facilitate the coupling. The hierarchical scheme is further divided into serial, embedded and equation-free scheme based on the knowledge about macroscopic models. The corresponding multiscale methods are reviewed and compared. In addition, the coupling of time scales is discussed for the multiple-time-scale simulations. Finally, some issues and further developments about multiscale simulations are discussed, which include the terminology, spatial and temporal scale separation, the roles of mesoscopic methods and domain decomposition, the reduced-order models and the future applications.

Contents

* Corresponding author.
E-mail address: yalinghe@mail.xjtu.edu.cn (Y.-L. He).

https://doi.org/10.1016/j.ijheatmasstransfer.2019.04.004
0017-9310/

1. Introduction

Many problems in the field of thermo-fluid science and engineering contain phenomena in different spatial and temporal scales. These problems are called multiscale problems. To mention some typical examples, the thermal management in the data center is a multiscale problem [1]. The heat transfers through multiple length scales, which contain the chip, server, rack and room with length scales ranging from centimeters to tens of meters. The mass transport processes in geologic formations are also multiscale in nature, such as the geologic CO_2 sequestration and the production of shale gas [2–5]. The pores and fractures of geologic formations are in the scales from nanometers to micrometers, so the transport mechanisms are different. When the reservoir or the whole site are considered, the length scale of the problem can even extend to kilometers. Similar multiscale mass transfers and reactions can be found in fuel cells [6,7], in which the electrochemical reaction on the catalyst, diffusion in porous electrodes and mass transfer in fuel channels range from nanoscale to macroscale. Multiscale problems are also seen in the field of aeronautics and space engineering. The air flow around the space vehicles experiences different characteristic length scales when the rarefaction of the surrounding air changes during the launch and re-entry processes. The heat transfer inside the thermal insulation materials that protect the vehicles is also multiscale. For example, the silica aerogel is mainly composed of nanoscale solid skeleton and porous networks, but is also doped with opacifiers and reinforced with fibers in micrometers [8].

It is not exaggerating to claim that the multiscale hierarchical structure is the nature of science [9] and our descriptions of the phenomena change when we view the phenomena from different scales. The reductionism leads to the searching for microscale fundamental laws that extend the universality of the theory. Although the macroscopic behavior ultimately obey the microscopic laws, it is impractical to make macroscopic predictions from microscopic laws because of the huge amount of computation. On the other hand, the macroscopic descriptions are closer to engineering applications, but the microscopic details are filtered and the empirical or phenomenal assumptions are introduced. Therefore, the models from a single scale are not sufficient for the multiscale problems. The multiscale models are needed to better understand the processes in different scales.

This paper focuses on the multiscale numerical methods for the modeling of problems in heat transfer and fluid flow as mentioned above. The numerical methods in the macroscale, mesoscale and microscale have been widely studied and implemented in this field. Much effort has also been made to build the multiscale models which connect and combine the models in different scales. However, currently the multiscale models are usually proposed for particular problems, and the techniques for the construction of multiscale models usually focus on the connection between specific models. In order to further develop the multiscale models, it is the time to have an overview of the current state of the multiscale models. The general multiscale frameworks and coupling strategies should be summarized to inspire the construction of the multiscale models. The direction of the further developments should be also clarified based on the survey of the current state of progress. These are the main objectives of the present review.

The rest of the paper is organized as follows. In Section 2 the numerical methods in macroscale, mesoscale and microscale are briefly reviewed as the foundation of the multiscale models. Then the multiscale frameworks for multiscale methods are reviewed and summarized in Section 3. The multiscale methods are mainly divided into domain decomposition scheme and hierarchical scheme, and the two categories are discussed respectively in the following two sections. Section 4 focuses on the key problem of the domain decomposition scheme: the information exchange between different numerical methods. The coupling techniques between numerical methods mentioned in Section 2 are reviewed. In Section 5, the hierarchical scheme is further divided into serial, embedded and equation-free schemes and the schemes are discussed separately. The coupling between temporal scales is specially discussed in Section 6. Finally, some discussions about some issues in multiscale simulations and the future developments are presented.

2. Numerical method in different scales

2.1. Macroscopic numerical methods

The foundations of macroscopic numerical methods are the macroscopic governing equations based on the continuum hypothesis [10]. Here the fluid is considered to be continuous and the

macroscopic properties are well-defined in the sensitive volume. The sensitive volume contains enough number of molecules, so the microscopic fluctuations have no effects on the macroscopic properties. The sensitive volume is also small comparing to the macroscale of observation, so the properties can be defined "locally and continuously", and their derivatives are meaningful as well. Then, the governing equations are established from the fundamental physical laws: the conservations of mass, linear momentum and energy [11]:

$$\frac{\partial \rho}{\partial t} + \nabla \cdot (\rho \mathbf{u}) = 0 \tag{1}$$

$$\rho \frac{D\mathbf{u}}{Dt} = -\nabla \cdot \mathbf{\Pi} + \rho \mathbf{f} \tag{2}$$

$$\rho \frac{D}{Dt}\left(\hat{U} + \frac{1}{2}u^2\right) = -\nabla \cdot \mathbf{q} - \nabla \cdot (\mathbf{\Pi} \cdot \mathbf{u}) + \rho Q + \rho(\mathbf{u} \cdot \mathbf{f}) \tag{3}$$

Here the denotations are density ρ, velocity $\mathbf{u}$, time t, stress tensor $\mathbf{\Pi}$, external body force $\mathbf{f}$, internal energy $\hat{U}$, heat flux $\mathbf{q}$, and heat source Q. The material derivative is given by $D/Dt = \partial/\partial t + \mathbf{u} \cdot \nabla$. The stress tensor can be decomposed into a pressure term $p\mathbf{I}$ and a deviatoric stress tensor $\boldsymbol{\tau}$: $\mathbf{\Pi} = p\mathbf{I}$-$\boldsymbol{\tau}$.

The above conservation equations are not closed because there are more unknown variables than the equations. Therefore, supplementary relations are needed to close the equations. One of the relations is the equation of state (EOS): $\hat{U} = \hat{U}(\rho, T)$, in which T is the temperature. The others are constitutive laws, which relate the flux $\mathbf{\Pi}$ and $\mathbf{q}$ to the state variables ρ, $\mathbf{u}$ and T and their derivatives. The constitutive laws can be constructed either "top-down" or "bottom-up". In the "top-down" procedure, the forms of the constitutive laws are constructed based on the considerations of symmetry, Galilean invariance, linearization and the second law of thermodynamics [12]. In the "bottom-up" procedure, the constitutive laws are derived from molecular theories such as the Boltzmann equation [13]. The well-known constitutive laws are Newton's law of viscosity and Fourier's law of heat conduction:

$$\boldsymbol{\tau} = \mu\left[\nabla \mathbf{u} + (\nabla \mathbf{u})^{\mathrm{T}}\right] + \left(\zeta - \frac{2}{3}\mu\right)\nabla \cdot \mathbf{u} \tag{4}$$

$$\mathbf{q} = -\kappa \nabla T \tag{5}$$

Here μ and ζ are the dynamic and bulk viscosity coefficients, and κ is the thermal conductivity.

In addition, the initial and boundary conditions are needed for the solving of governing equations. For the macroscopic problems, the non-slip velocity boundary conditions are widely adopted. Also, the fluid temperature is assumed to be the same as solid temperature on the boundary.

The macroscopic numerical methods are constructed to solve the governing equations. The typical methods are based on meshes. A numerical grid is generated, and the governing equations are discretized in space and time to obtain a set of algebraic equations of the variables at the grid points. Different methods have different ways to generate the discrete equations [14]. Typical numerical methods include the Finite Difference Method (FDM), Finite Volume Method (FVM) [14], and Finite Element Method (FEM) [14,15]. After the discretization procedures, the numerical algorithms such as the SIMPLE [16] are used to solve the set of algebraic equations. Besides the mesh-based methods, there are also different kinds of mesh-free methods such as the smoothed particle hydrodynamics (SPH) [17–19].

Since the governing equations, constitutive laws, initial and boundary conditions are the basis for macroscopic methods, the macroscopic methods are not valid when these macroscopic assumptions and models fail. It should be mentioned that it is usually the failure of constitutive laws or boundary conditions that break the macroscopic descriptions. For example, in the rarefied gas flows or micro/nanoscale flows, when the characteristic length of flow is comparable to the mean-free-path, the continuum hypothesis is not valid and special boundary phenomena such as the velocity slip and temperature jump should be considered [20]. Another problem of the macroscopic methods is the determination of the empirical parameters of the constitutive laws, such as the viscosities, can be difficult. For complex fluids such as the polymeric fluids, the constitutive law for stress will become quite complicated, and the physical meaning of the fitted parameters will be obscure [21]. Therefore, the numerical method on more fundamental basis are needed to provide the parameters, constitutive laws and boundary conditions to the macroscopic methods, or to conduct simulations without the empirical assumptions.

2.2. Microscopic molecular dynamics

Instead of building models from macroscale continuum hypothesis, the models can be also established directly from microscale. In classical molecular dynamics (MD), the motion of every atom (or molecule) is simulated and the motion is described by Newton's second law as:

$$m_i \frac{d^2 \mathbf{r}_i}{dt^2} = \mathbf{F}_i \tag{6}$$

m_i is the mass of the ith atom, $\mathbf{r}_i$ is the location and $\mathbf{F}_i$ is the total force acting on the atom. The interaction between atoms is described by potential functions, and the Lennard-Jones (L-J) potential is widely used:

$$\varphi(r_{ij}) = 4\varepsilon\left[(\sigma/r_{ij})^{12} - (\sigma/r_{ij})^{6}\right] \tag{7}$$

The r_{ij} is the distance between atoms i and j, and the ε and σ determine the strength and length of the interaction. In practice a cut-off distance r_c is used so that the interaction is considered only when $r_{ij} < r_c$. Modification of potential could be made to guarantee the continuity of potential and force at r_c [22,23]. Then, the force that atom j acts on atom i is given by $\mathbf{F}_{ij} = -\partial\varphi(r_{ij})/\partial\mathbf{r}_i$. The $\mathbf{F}_i$ is the summation of all the interatomic forces $\mathbf{F}_{ij}$ and the external force $\mathbf{F}_i^{\mathrm{ex}}$. Since Eq. (6) should be solved in discrete time steps, a proper numerical scheme such as the Leapfrog scheme and predictor–corrector scheme should be chosen [22,24].

The computational domain is divided into cells or control volumes, and the macroscopic variables such as the density ρ, velocity $\mathbf{u}$, stress tensor $\mathbf{\Pi}$ and temperature T are then calculated from the ensemble average:

$$\begin{aligned}
\rho &= \tfrac{1}{V_{\mathrm{CV}}}\left\langle \textstyle\sum_{i=1}^{N} m_i \right\rangle_{\delta t} \\
\rho\mathbf{u} &= \tfrac{1}{V_{\mathrm{CV}}}\left\langle \textstyle\sum_{i=1}^{N} m_i \mathbf{v}_i \right\rangle_{\delta t} \\
\mathbf{\Pi} &= \tfrac{1}{V_{\mathrm{CV}}}\left\langle \textstyle\sum_{i=1}^{N} m_i(\mathbf{v}_i - \mathbf{u})(\mathbf{v}_i - \mathbf{u}) + \sum_{i=1}^{N}\sum_{j>i}^{N} \mathbf{r}_{ij}\mathbf{F}_{ij} \right\rangle_{\delta t} \\
T &= \left\langle \tfrac{1}{3Nk_{\mathrm{B}}} \textstyle\sum_{i=1}^{N} m_i |\mathbf{v}_i - \mathbf{u}|^2 \right\rangle_{\delta t}
\end{aligned} \tag{8}$$

Here $\langle\cdot\rangle_{\delta t}$ is the time average in interval δt, V_{CV} is the volume of the cell, and N is the number of atom inside the control volume in interval δt. $\mathbf{v}_i$ is the velocity of atom and k_{B} is the Boltzmann constant. It can be seen that the basic molecular dynamics is based on microcanonical (NVE) ensemble. In order to achieve constant temperature or constant pressure in the simulation, thermostatic or constraint methods should be applied [22,24].

Since the motions of all the molecules are modelled in the MD simulations, the length and time scale of the MD simulations are rather limited. The typical scales are nanometers and picoseconds.

Therefore, it is unrealistic to apply pure MD simulations to macroscopic engineering problems. However, the MD can be used to study the fundamental microscale mechanisms as the supplementary to the macroscopic methods. Then the multiscale methods are needed.

2.3. Particle-based mesoscopic methods

In molecular dynamics, the position, velocity and interaction of every atom or molecule are known. However, the above excessively detailed information is not necessary if the interest of research is only the macroscopic behavior of the system. Then, the models in more coarse-grained scale are preferred. In the coarse-grained models, computational particle can be used to represent a group of molecules. By constituting proper evolution mechanisms of the particles, the macroscopic behavior can be recovered without the detailed information of every molecule. When dissipative force and random perturbation are added to the conservative force between particles to mimic the hydrodynamic behavior, we get the dissipative particle dynamics (DPD). When the motion of particles are discrete in discrete velocity, spatial and temporal space and the collision rules are simplified, we get the lattice gas automata (LGA) and the lattice Boltzmann method (LBM). When the collision between particles are represented by probabilistic sampling, we get the direct simulation Monte Carlo (DSMC) method. These are the typical examples of the particle based methods [25]. Comparing with the macroscopic governing equations and constitutive laws which are based on the continuum assumption, these particle-based methods are still in the discrete level with smaller spatial and temporal scales. On the other hand, the coarse-grained particles have much larger scales than the microscopic molecules. Therefore, they can be regarded as mesoscopic methods. Since Boltzmann equation is the basis of both DSMC and LBM, in the following sections a brief introduction to the Boltzmann equation is given firstly and the introductions to these mesoscopic methods are followed.

2.3.1. Boltzmann equation

The Boltzmann equation can be written as [13,26,27]:

$$\frac{\partial f}{\partial t}+\mathbf{c}\cdot\frac{\partial f}{\partial \mathbf{x}}+\mathbf{F}\cdot\frac{\partial f}{\partial \mathbf{c}}=\int_{-\infty}^{\infty}\int_{0}^{4\pi}\left(f'_1f'-f_1f\right)g\sigma d\Omega d\mathbf{c}_1 \tag{9}$$

It describes the evolution of distribution functions $f(\mathbf{x}, \mathbf{c}, t)$. Here we assume that f is the mass density distribution instead of the number density distribution. The mass of all the molecules at time t, located in the volume element $[\mathbf{x}, \mathbf{x}+d\mathbf{x}]$ and with velocities in the range $[\mathbf{c}, \mathbf{c}+d\mathbf{c}]$, equals $f(\mathbf{x}, \mathbf{c}, t)d\mathbf{x}d\mathbf{c}$. Similarly to Eq. (8) the macroscopic variables are the moments of f with respect to $\mathbf{c}$ and $\mathbf{C}=\mathbf{c}-\mathbf{u}$ [26]. The $\mathbf{F}$ in Eq. (9) is an external body force, so the left-hand side of Boltzmann equation is the evolution of f in a phase-space consisted of spatial and velocity coordinates. The right-hand-side is an integral term representing the contributions from two-body collisions. Here two molecules with velocities $\mathbf{c}$ and $\mathbf{c}_1$ collide and the after-collision velocities are $\mathbf{c}'$ and $\mathbf{c}'_1$. The corresponding velocity distribution functions are $f(\mathbf{x},\mathbf{c},t)$, $f_1(\mathbf{x},\mathbf{c}_1,t)$, $f'(\mathbf{x},\mathbf{c}',t)$ and $f'_1(\mathbf{x},\mathbf{c}'_1,t)$. The g is the relative velocity $|\mathbf{c}\text{-}\mathbf{c}_1|$, $d\Omega$ is the element of solid angle and σ is the differential cross-section which is determined by the potential between molecules. In the equilibrium state the collision term should vanish, and one can derive the Maxwell equilibrium distribution function $f^{\mathrm{eq}}=\rho(m/2\pi kT)^{3/2}\exp\left(-mC^2/2kT\right)$.

It can be seen that the Boltzmann equation is a complex nonlinear integro-differential equation which is hard to solve. The Chapman-Enskog method and Grad's moment method are two typical methods for solving the Boltzmann equation [13,26,28]. There are three characteristics of the solution of Boltzmann equation that are important to the coupling with macroscopic and mesoscopic methods.

Firstly, in the absence of external body force, the Boltzmann equation can be rescaled into [26]:

$$Sr\frac{\partial f^*}{\partial t^*}+\mathbf{c}^*\cdot\frac{\partial f^*}{\partial \mathbf{x}^*}=\frac{1}{Kn}\int_{-\infty}^{\infty}\int_{0}^{4}\left(f_1^{*'}f^{*'}-f_1^*f^*\right)g^*\sigma^*d\Omega^*d\mathbf{c}_1^* \tag{10}$$

Here the * represents dimensionless variables. The Strouhal's number is $Sr=L_c/\bar{c}\,t_c$, where L_c and t_c are the characteristic length and time of the flow. The important Knudsen's number Kn is defined as the ratio between mean free path λ and L_c:

$$Kn=\lambda/L_c \tag{11}$$

It can be seen in Eq. (10) that Kn determines the importance of the collision term on the gas flow. Therefore Kn measures the degree of rarefaction of gases. It also measures the relative importance of the collision between molecules and the collision between molecule and boundary [20]. The $Kn < 0.001$ is the continuum flow regime in which the macroscopic Navier-Stokes (N-S) equations and non-slip boundary conditions can be used. The $0.001 < Kn < 0.1$ is the slip-flow regime in which the N-S equations are still valid for the bulk flow but the boundary slip should be considered. The $0.1 < Kn < 10$ is the transition regime. The continuum assumption is no longer valid and the Boltzmann equation should be solved for the flow. When $Kn > 10$, the collision between molecules can be neglected and it is the free-molecular regime. Therefore, the Kn is an index to show when the continuum models are not valid and the mesoscopic/microscopic models and multiscale models are needed.

Secondly, the Chapman-Enskog method and Grad's moment method generate the relations between velocity distribution functions and the macroscopic variables, which are important for the information transfer between different numerical methods. In Chapman-Enskog method, the distribution function f is expanded in power series of a parameter ε which is comparable to Kn:

$$f=f^{\mathrm{eq}}+\varepsilon f^{(1)}+\varepsilon^2 f^{(2)}+\cdots \tag{12}$$

The $f^{(1)}$ and $f^{(2)}$ are the deviations from the equilibrium distribution function and they can be represented by macroscopic variables and their gradients. The Euler equations, N-S equations and Burnett equations can be recovered with increasing orders of the approximation. In Grad's moment method, the distribution function is expanded into series of tensorial Hermite polynomials $H_{i_1\,i_2\cdots\,i_N}$ as [28,29]:

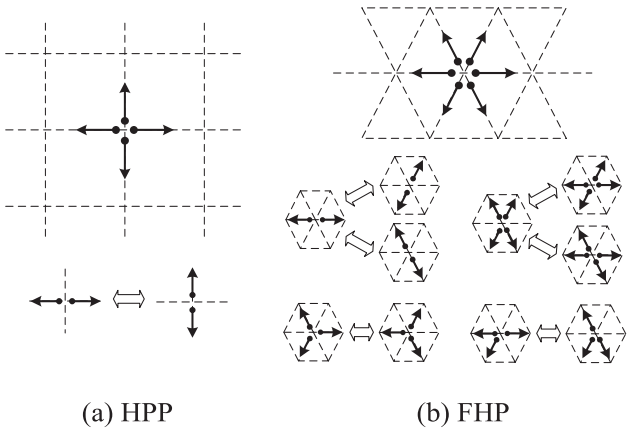

Fig. 1. Sketches of the LGA models.

$$f = f^{\mathrm{eq}}\left(aH + a_i H_i + \frac{1}{2!}a_{ij}H_{ij} + \cdots + \frac{1}{N!}a_{i_1\ i_2\ldots\ i_N}H_{i_1\ i_2\ldots\ i_N} + \cdots\right) \quad (13)$$

Here the $H_{i_1\ i_2\ldots\ i_N}$ are functions of the molecular peculiar velocity $\mathbf{C}$, and the coefficients $a_{i_1\ i_2\ldots\ i_N}$ are functions of macroscopic variables. By this expansion the Nth-order moments of the Nth-order polynomial distribution function are the same as those of the original distribution function. It can be seen that Eqs. (12) and (13) generate the relations between mesoscopic distribution functions and the macroscopic variables. Since the velocity distribution function is intrinsically related to the velocities of microscopic molecules, they can be a bridge between the methods in different scales.

Thirdly, the complex collision term can be simplified while the basic properties are still maintained. A well-known simplification is the BGK model [30], in which the collision is replaced by a relaxation process to the equilibrium distribution function with a relaxation time τ:

$$\frac{\partial f}{\partial t} + \mathbf{c}\cdot\frac{\partial f}{\partial \mathbf{x}} + \mathbf{F}\cdot\frac{\partial f}{\partial \mathbf{c}} = -\frac{f - f^{\mathrm{eq}}}{\tau} \quad (14)$$

This simple collision term has the same summational invariants with the original collision term and holds the H-theorem. The hydrodynamic equations can be also recovered from Eq. (14). It gains special interests in the mesoscopic methods because it is closely related to the LBM.

2.3.2. Direct simulation Monte Carlo

Boltzmann equation suggests that if the collision term on the right-hand-side is correctly modeled, one can reproduce the hydrodynamics behavior without the detailed simulation of every molecules. Therefore, in DSMC a statistical sampling of the collision is proposed to simplify the calculation of collision between every pair of molecules.

In DSMC the computational particles which represent groups of molecules are simulated. The computational domain is divided into cells and the macroscopic values are calculated in each cell similarly to the MD. The particles experience advection and collision processes in each time step Δt_{m}. In order to decouple the molecular motion with the collision, the Δt_{m} should be small in comparison with the local mean collision time [31]. Thus, the particles moves $\mathbf{v}_i\Delta t_{\mathrm{m}}$ according to their velocity $\mathbf{v}_i$ in the advection process, and then collide with each other according to the statistical sampling.

The collision step is manipulated cell by cell. In each cell random pairs of particles are selected firstly and the probability for the occurring of collision between each pair is $P_{\mathrm{col}} = g\sigma/(g\sigma)_{\max}$. Here the differential cross-section σ is a function of relative speed g and is determined by the specific molecule model and the potential that are used. $(g\sigma)_{\max}$ is the maximum value of $g\sigma$ in the cell. As for the number of the samplings of collision in each cell, Bird introduced the "time-counter" (TC) method [32] and later the "no-time-counter" (NTC) method [27] for the DSMC.

The limitation of DSMC is that its spatial and temporal scales must be resolved to the mean free path and mean collision time, and each cell should at least contain 20 particles [27]. Therefore, although the DSMC is an efficient method for rarefied gas flows, it becomes compute-intensive for the continuum flow regime when Kn is small.

2.3.3. Lattice gas automata and lattice Boltzmann method

In DSMC the collision between computational particles is statistically sampled, but the particles still moves in continuous velocity and spatial space. In the LGA model, the computational particles can only stay on the lattice nodes and jump to the neighbor nodes in a time step. The particles have a discrete set of velocity that is linked with the lattice vectors. For example, in the original HPP LGA model the regular square lattice is used [33,34]. The lattice velocities are $\mathbf{c}_i = c[\sin(i\pi/2),\ \cos(i\pi/2)]$, $i = 1$–4, as drawn in Fig. 1. If the space and time steps are Δx and Δt, the lattice speed is $c = \Delta x/\Delta t$, so the particles can move from one node to a neighbor node in a time step. At each node there are four cells corresponding to the four velocities and neighbor nodes. Each cell can only be empty or occupied by one particle, so it is a Boolean variable. In a more symmetric FHP model [35], the hexagonal lattice is used. Each node has six cells with lattice velocities $\mathbf{c}_i = c[\sin(i\pi/3),\ \cos(i\pi/3)]$, $i = 1$–6.

Then, similar to the DSMC, the evolution of LGA can be divided into two processes: collision and propagation. In the propagation process the after-collision occupations move to the neighbor nodes corresponding to the directions of the velocities. In the collision process the occupation states of the cells at a node are changed according to the collision rule, which is based on the conservation of mass, momentum and energy. As shown in Fig. 1, the collision rule for HPP model is simple. When two particles with opposite velocity enter a node, rotate both particles by 90°. However, for FHP model the collision rule is more complex because each node contains 2^6 states and totally 2^{12} possible state transition should be considered in the implementation. Finally, the macroscopic values in LGA are also calculated by ensemble average in each node.

The LGA has many advantages such as the absolute stability, easy boundary condition implementation and intrinsic parallelism. However, it also suffers many problems including statistical noise, violation of the Galilean invariance, exponential complexity of collision operator and spurious invariants. The remedies of these diseases lead to the dawn of the LBM [36–38]. The therapies include continuous distributions instead of Boolean variables [39], linearized collision operators [40,41] and Boltzmann distribution instead of Fermi-Dirac distribution. Finally, the milestone of this transformation is a simple collision operator with BGK approximation [30], and the most widely used single-relaxation-time LBM (also called LBGK model) is constructed [42–46].

Qian et al. [43] proposed a family of LBGK model with b velocities on d-dimensional simple cubic lattice (called DdQb model). The evolution equation without external force is

$$f_i(\mathbf{x} + \mathbf{c}_i\Delta t, t + \Delta t) - f_i(\mathbf{x}, t) = -\frac{f_i(\mathbf{x}, t) - f_i^{\mathrm{eq}}(\mathbf{x}, t)}{\tau} \quad (15)$$

Here f_i is the discrete distribution function and the equilibrium distribution f_i^{eq} is given by:

$$f_i^{\mathrm{eq}} = \rho w_i\left[1 + \frac{\mathbf{c}_i\cdot\mathbf{u}}{c_s^2} + \frac{(\mathbf{c}_i\cdot\mathbf{u})^2}{2c_s^4} - \frac{u^2}{2c_s^2}\right] \quad (16)$$

in which w_i are the weighting factors and c_s is the lattice sound speed. The macroscopic variables can be therefore calculated from the moments of f_i:

$$\begin{aligned} &\rho = \textstyle\sum_{i=0}^{b-1} f_i \\ &\rho\mathbf{u} = \textstyle\sum_{i=0}^{b-1} \mathbf{c}_i f_i \\ &\boldsymbol{\tau} = \rho\nu\left[\nabla\mathbf{u} + (\nabla\mathbf{u})^{\mathrm{T}}\right] = -\left(1 - \tfrac{1}{2\tau}\right)\textstyle\sum_{i=0}^{b-1}\mathbf{c}_i\mathbf{c}_i(f_i - f_i^{\mathrm{eq}}) \end{aligned} \quad (17)$$

in which $\boldsymbol{\tau}$ is the deviatoric stress tensor of LBM. The LBGK model has an equation of state $p = \rho c_s^2$. With the Chapman-Enskog expansion procedure, it can be shown that the LBGK model can reproduce N-S equation in the nearly-incompressible limit [38], and the relation between kinematic viscosity ν and τ is $\nu = c_s^2(\tau - 1/2)\Delta t$. Taking the most common D2Q9 model as an example, the discrete velocities are $\mathbf{c}_0 = c(0,0)$, $\mathbf{c}_{1\sim4} = c(\pm1,0)$, $c(0,\pm1)$ and $\mathbf{c}_{5\sim8} = c(\pm1,\pm1)$. The weighting factors are $w_0 = 4/9$, $w_{1\sim4} = 1/9$ and $w_{5\sim8} = 1/36$ and the lattice sound speed is $c_s = c/\sqrt{3}$.

Although the LBM is historically evolved from LGA, quickly it is found that the LBM can be derived from continuum Boltzmann BGK Eq. (14) directly [47–50], and finally the systematic procedures for building higher-order LBM from continuum Boltzmann BGK equation by Hermite expansions and Gauss–Hermite quadrature are proposed [51,52]. Therefore, the LBM has a rigorous kinetic theory basis and inherits several advantages of LGA as a particle-based method, such as the simple implementation of complex boundary condition and parallel computing. It is also an explicit time marching scheme and does not need to solve systems of discrete equations simultaneously. In the past two decades, both the theories and applications of LBM have been extensively expanded, and it has been developed into a powerful numerical method for a wide range of problems. Several recent review papers about LBM can be suggested to the readers [53–57].

Meanwhile, the LBM still has drawbacks comparing with the continuum method. As a natural-born dynamic scheme, LBM is not a method of choice for steady state problems [53,57]. Its efficiency is further limited by small Δt, because the nearly-incompressible limitation requires a large lattice sound speed $c_s = \Delta x/\Delta t\sqrt{3}$ [58,59]. However, LBM is more efficient than continuum methods for unsteady problems when the time steps of LBM and continuum methods are the same, or when it is used in complex geometries [58–60]. Thus a multiscale method combining LBM with continuum methods is promising.

2.3.4. Dissipative particle dynamics and smoothed dissipative particle dynamics

The other modification of MD is the DPD method, in which the friction effects are added to the interactions to mimic the hydrodynamic behavior. In the DPD method the motion of particle is also described by Newton's law, but a dissipative force $\mathbf{F}_{ij}^{\mathrm{D}}$ and a random force $\mathbf{F}_{ij}^{\mathrm{R}}$ are added besides the conservative interaction force [61–64]. The motion equations are:

$$\frac{d\mathbf{r}_i}{dt} = \mathbf{v}_i \tag{18}$$

$$m_i \frac{d\mathbf{v}_i}{dt} = \sum_{j\neq i} \mathbf{F}_{ij}^{\mathrm{C}} + \sum_{j\neq i} \mathbf{F}_{ij}^{\mathrm{D}} + \sum_{j\neq i} \mathbf{F}_{ij}^{\mathrm{R}} \tag{19}$$

Here the $\mathbf{F}_{ij}^{\mathrm{C}}$ is still the conservative force between particles, and a soft repulsion force is usually adopted, in which $\mathbf{F}_{ij}^{\mathrm{C}} = a_{ij}(1-r_{ij})\hat{\mathbf{r}}_{ij},\ r_{ij}<1$ and $\mathbf{F}_{ij}^{\mathrm{C}} = 0,\ r_{ij}\geqslant 1$. Here $\mathbf{r}_{ij} = \mathbf{r}_i - \mathbf{r}_j$ and $\hat{\mathbf{r}}_{ij} = \mathbf{r}_{ij}/r_{ij}$. The cut-off distance is assumed to be unit. The dissipative force and random force are give by $\mathbf{F}_{ij}^{\mathrm{D}} = -\gamma w^{\mathrm{D}}(r_{ij})(\hat{\mathbf{r}}_{ij}\cdot\mathbf{v}_{ij})\hat{\mathbf{r}}_{ij},\ \mathbf{F}_{ij}^{\mathrm{R}} = -\sigma w^{\mathrm{R}}(r_{ij})\zeta_{ij}\hat{\mathbf{r}}_{ij}$. Here $\mathbf{v}_{ij} = \mathbf{v}_i - \mathbf{v}_j$. $w^{\mathrm{D}}$and w^{R} are weight functions and γ and σ are coefficients. ζ_{ij} is a Gaussian white-noise term.

It can be seen that the dissipative force is proportional to the momentum differences and tends to relax the relative motion, while the random force keeps the system in motion. The symmetry of force terms conserves the system's momentum. Since the force terms are only related to the relative position and relative velocity, DPD is Galilean invariant [65]. Also, the fluctuation in mesoscale is naturally included in DPD, so DPD is a promising method for the simulation of mesoscopic complex molecules and fluid systems. It has been applied in a variety of research fields such as colloids, polymers, blood flows, and liquids with interfaces [64–66].

However, the original DPD has some disadvantages including the difficulties in applying arbitrary equations of state and specifying the transport coefficients directly. It is also absent of a physical scale. The smoothed dissipative particle dynamics (SDPD) proposed by Español and Revenga can prevent these drawbacks [67]. In contrast with DPD which is built bottom-up from the interaction of particles, the SDPD is constructed top-down from Lagrangian description of Navier-Stokes equations. In SDPD each particle can be regarded as a moving thermodynamic subsystem with mass, entropy and volume. The volume is calculated from weight functions which include a smoothing length h that control the size of the particle and the scale of the simulation [67–69]. The thermodynamics are also introduced by choosing an internal energy function for the particles. Finally, by casting the model in GENERIC framework, the DPD-like thermal fluctuations can be also introduced into the model [64].

Since the SDPD is constructed from a top-down perspective, both the equations of state and transport coefficients can be specified as inputs of the model. Also, the model maintains the important mesoscopic fluctuation feature. By defining a volume for each particle, a physical scale h is specified. The effects of thermal fluctuation increase with the decreasing of the scale. Therefore, the SDPD solves the drawbacks of the DPD. This top-down approach leads to the flexibility to extend the method to multicomponent problems [68]. The specified scale also facilitates the multiscale method based on SDPD [68,69], which will be discussed in Section 4.2.2.

3. Multiscale frameworks

From the aforementioned introductions of the numerical methods in different scales it can be seen that a method in single scale is not sufficient for the multiscale simulations. Therefore, multiscale numerical methods are needed. Although the multiscale simulations are widely studied in a variety of disciplines, there are still a lot of problems that are needed to be clarified, such as the terminology, the classification of multiscale models and the modeling strategies [70]. Therefore, in this section the framework of the multiscale method is summarized and established based on the survey and analyses of the existing researches.

Focusing on different aspect of multiscale methods, some classifications and frameworks has been proposed. For example, Ingram et al. [71] summarized five types of coupling frameworks for multiscale simulations: Multidomain, Embedded, Parallel, Serial and Simultaneous. Different types have different computational domain allocations and information transfer schemes. E et al. [21,72–76] classified the multiscale problems according to whether the microscopic descriptions are needed locally or globally. They distinguished the serial and "on-the-fly" concurrent coupling strategies for the information exchange. A Heterogeneous Multiscale Method (HMM) was also proposed as a general framework for the multiscale problems, which consists of an overall macroscopic model and the microscopic models which provide the missing data for the macroscopic model. In HMM the macroscopic model should have been known to some extent. In contrast, the framework "Equation-Free" Multiscale Method (EFM) proposed by Kevrekidis et al. [77,78] aims to perform macroscale simulations directly from microscopic methods without having a macroscopic level closed description. The main point of the EFM is to extract information in macroscale from short bursts of microscopic simulations in space and time. Aiming at the multiscale hydrogeologic modeling, Scheibe et al. [79] proposed a flowchart called "Multiscale Analysis Platform (MAP)" as a framework for the chosen of multiscale methods. By asking a series of questions which include the degree of coupling, the spatial and temporal scale separation, the percentage of the small scale region and the knowledge about the macroscopic model, the MAP will lead the modeler to a specific motif. Borgdorff, Chopard and Hoekstra et al. [80–82] also proposed a systematic Multiscale Modeling and Simulation Framework (MMSF) for the multiscale computation. The MMSF contains the definition and classification of

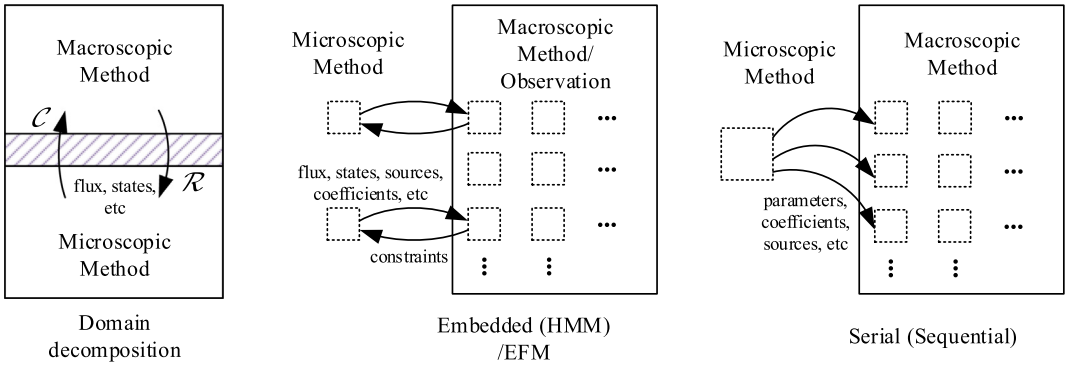

Fig. 2. Sketches of the computational domains for different multiscale numerical methods.

multiscale problems, the execution loop of sub-models, and the templates and topology of coupling procedures. Based on MMSF, a multiscale coupling environment is also established and the distributed computation strategies are proposed [83,84]. Yang and Marquardt [85] used set-theoretic langrage to build an ontological conceptualization framework of multiscale models. They also demonstrated that the other existing frameworks can be described and clarified by their conceptualization.

The above mentioned multiscale frameworks are general for the multiscale simulations in in different disciplines. There are also other frameworks specifically proposed for the multiscale simulations of fluid flow and heat transfer. Kalweit et al. [86] and Drikakis et al. [87] proposed a graph for the classification of hybrid particulate-continuum methods. The methods are primarily categorized into domain-decomposition approach and point-wise-coupling approach. The domain-decomposition is composed of state-coupling and flux-coupling, while the point-wise-coupling approach contains EFM and HMM. He and Tao [88,89] divided the multiscale problems into multiscale system and multiscale process. For the multiscale system, the phenomena in different scales are described by the same governing equations and can be solved by the same numerical methods. The top-to-down serial simulation method with increasing fineness of grid is suggested for this kind of problem. On the contrary, in multiscale process the phenomena in different scales are described by different governing equations and different numerical methods are needed. For the information exchange between different scales, the concepts of compression operator and reconstruction operator were used. They pointed out that the establishment of reconstruction operator is more difficult because the microscale contains more information.

The brief survey of the existing frameworks shows a diversity of the terminology and classification of the multiscale methods. The reason is that the authors focus on specific topics and aspects of the multiscale simulation. However, the frameworks are still consistent with each other in most of the aspects.

First of all, the multiscale methods are similarly classified into the following categories: domain decomposition (multidomain), serial (sequential, individual), embedded (HMM), and equation-free. Also, the spatial scale separation is a precondition for most of the multiscale methods. The domain decomposition requires a small region of microscopic descriptions, and the serial, HMM and EFM take advantages of representative elementary volume. Otherwise, the microscopic models should be applied to the whole computational domain, and the traditional multiresolution methods are needed. The simulation can also take advantages of self-similarity [79]. The multiresolution is generally not in the scope of multiscale method and the fractal-methods for self-similarity is not a common method for the multiscale simulations of flow and heat transfer. Therefore, we will focus on the multiscale methods with scale separation in the present work.

Secondly, the domain decomposition method is mentioned in most of the researches and distinguished from other methods. The biggest difference is that both the macroscopic and microscopic methods span a part of the computational domain in the domain decomposition. Although small hand-shaking region can be employed for the information transfer, the rest of the computational domain is simulated by either macroscopic or microscopic methods without overlap. In the other categories the macroscopic methods span the whole domain while the microscopic methods are pre-computed separately or embedded point-wisely in small regions as supplements to the macroscopic methods. The computational domains for different multiscale methods are shown in Fig. 2. The term macroscopic observation is used specially for EFM, in which there are no macroscopic models but the observation of macroscopic behavior is adopted in the whole domain.

Thirdly, Fig. 2 shows that the serial, embedded and EFM have similar computational domains. Analyses of the methods demonstrate that the main difference among the methods is the knowledge about the models [21]. As mentioned in Section 2.1, the macroscopic models are mainly composed of governing equations and constitutive laws (boundary conditions). The serial method is based on the well-established governing equations and constitutive laws (boundary conditions), such as Eqs. (1)–(3) and Eqs. (4), (5). Therefore, the macroscopic models and microscopic models can be fully decoupled, and one can simply use separate microscopic simulations to determine the coefficients for the macroscopic models. The information transfer is one-way. However, when the constitutive laws are too complex and many coefficients, variables, gradients are involved, or when there is no close forms for constitutive laws, the unknown terms in the governing equations such as the stress, heat flux and heat source should be calculated from the microscopic simulations "on-the-fly". The "two-way" information exchange between macroscale and microscale is employed during the whole computation. An extreme condition is the EFM, in which even the macroscopic equations are not clear, and the simulations are conducted directly from microscopic models.

Finally, although the temporal coupling schemes are proposed separately for different frameworks, the schemes are general for almost all the multiscale methods. The temporal scale separation is a criterion for the scheme. If the relaxation time of microscopic process is much smaller than the macroscopic process, the microscopic simulations can be adopted in short time bursts and the macroscopic values can be obtained by temporal extrapolations. On the other hand, if there is no temporal scale separation, the time parallel scheme should be used and the simulation time of microscopic simulation should extend to the whole time of the simulations. Also, a seamless method is initially proposed for

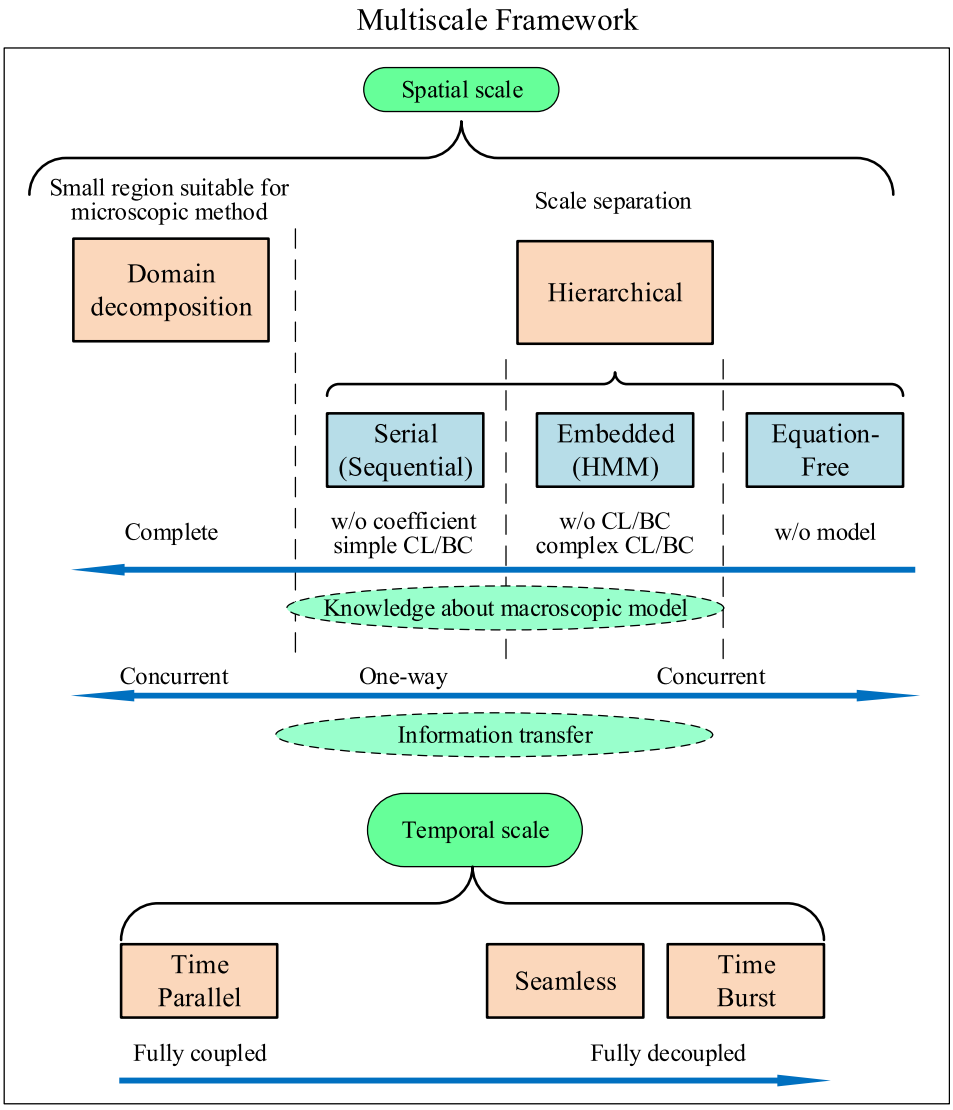

Fig. 3. Framework for multiscale methods (CL for constitutive laws, BC for boundary conditions, HMM for heterogeneous multiscale method, w/o for without).

HMM, in which the macroscopic and microscopic methods use different time steps [90–93]. It will be shown later that the seamless scheme has the potential to be extended to other multiscale simulations.

Based on the above discussions, the classification and frameworks for the multiscale methods are summarized in the present work and shown in Fig. 3. Firstly, the domain decomposition method and hierarchical methods are distinguished. The hierarchical methods are based on the spatial scale separation. For the domain decomposition, we argue that the selection criterion is that the sub-region for microscopic methods is small and suitable for the microscopic methods. Then, the hierarchical methods are further decomposed into serial methods, embedded methods and equation-free methods based on the knowledge about macroscopic models. We also added that the domain decomposition method needs a complete knowledge about macroscopic models. Furthermore, the information transfer schemes are also noted in the framework, in which the serial methods use on-way transfer and the other methods adopt concurrent coupling with two-way transfer. Finally, the temporal scale coupling is divided into fully coupled with time-parallel methods and fully decoupled with time-burst method. The seamless method also requires a temporal scale separation, thus it is close to the time-burst method.

For the completeness of the discussion, we further discuss the coupling schemes for the multiscale methods. The main scheme is inspired by the scheme proposed by E et al. [21,76] for HMM. The macroscopic and microscopic variables are denoted by U and u, and they are mutually transformed by operators $\mathcal{R}$ and $\mathcal{C}$ as: $u = \mathcal{R}U$, $U = \mathcal{C}u$. The operator $\mathcal{R}$ is called reconstruction operator or lifting operator, while $\mathcal{C}$ is called compression operator or restriction operator [21,77]. The operators can be either mathematical relations or numerical treatments for information transfer. The complexity of $\mathcal{R}$ is generated from the asymmetry of information between U and u. Since microscale contains more information than the macroscale, the $\mathcal{R}$ is a one-to-many mapping and it is not unique. A good $\mathcal{R}$ should be physically meaningful, mathematically stable, computationally efficient, and easy to be implemented [88,89,94]. Meanwhile, the operators need to obey the relation $\mathcal{QR} = \mathcal{I}$. Here $\mathcal{I}$ is an identity operator. We cannot expect the two operators are commutative and usually $\mathcal{RQ} \neq \mathcal{I}$ because the microscale information is filtered in $\mathcal{R}$. Then, the macroscopic and microscopic numerical models can be represented as [21]:

$$\partial_t U = F(U; D) \tag{20}$$

$$\partial_t u = f(u; d) \tag{21}$$

Here the D represents the missing data for the macroscopic models, such as the coefficients and boundary conditions, d is the data needed to update the microscopic models such as constraints or boundary conditions. Then, the coupling procedures generally consist of the following 4 steps: (1) Reconstruction; (2) Microscopic calculation; (3) Compression; (4) Macroscopic calculation.

Therefore, the framework for multiscale simulations is established and the coupling procedure is given. In the following sections, based on the multiscale framework, we will briefly review the researches on the domain decomposition multiscale methods, the hierarchical multiscale methods and the temporal coupling scheme, in order to further explain and exhibit the recent development of multiscale numerical methods for heat transfer and fluid flow problems.

It should be mentioned that although the numerical methods mentioned in Section 2 are divided into macroscopic, mesoscopic and microscopic methods, in the following discussions about general multiscale schemes, the term macroscopic method will refer to the numerical methods with relatively larger scale, and microscopic method will refer to methods with relatively smaller scale. For example, if the coupling between FVM and LBM is discussed, then the LBM will be called "microscopic" methods comparing with the FVM. This expression will not cause ambiguity due to the context.

4. Domain decomposition methods

The domain decomposition multiscale methods have been widely studied, and the coupling methods between almost all the numerical methods described in Section 2 are studied. The computational domain for domain decomposition coupling can be seen in the first picture of Fig. 2. The computational domain is divided into macroscopic and microscopic sub-regions which are solved by corresponding numerical methods. An overlapping region can be located between the two sub-regions for the convenience of information transfer. The boundaries of the sub-regions that need information transfer are called coupling boundaries in this work, where the reconstruction and compression operators are employed. Similarly to the Dirichlet and Neumann boundary conditions, the coupling can be based on state-exchange and flux-exchange, and the computational procedures for state-exchange coupling is therefore similar as the Schwarz alternating method [95].

Sometimes the coupling is not exactly described by this sketch. For example, in the coupling between LBM and DSMC, both methods are mesoscopic, so it is hard to clearly define the reconstruction and compression operators. In the coupling between MD and DPD/SDPD, the two methods are coupled by a gradual transition of interactive force. It is also hard to be characterized by state/flux-exchange. Still, the Fig. 2 is general in most of the situations.

4.1. Coupling between MD and continuum methods

The research on the coupling between MD and continuum methods for fluid system was pioneered by O'Connell and Thompson [96]. Since then, this topic has attracted many research attentions and inspired the coupling between other methods. Some comprehensive review papers about the hybrid molecular-continuum methods has been published [25,86,87,97]. Therefore, in this section we will briefly review the main ideas and components of the coupled MD-continuum methods.

4.1.1. Open boundary condition for MD

Since the coupling boundary of MD can exchange molecules with the continuum region in the domain decomposition simulations, one of the main problems for the MD is the open boundary

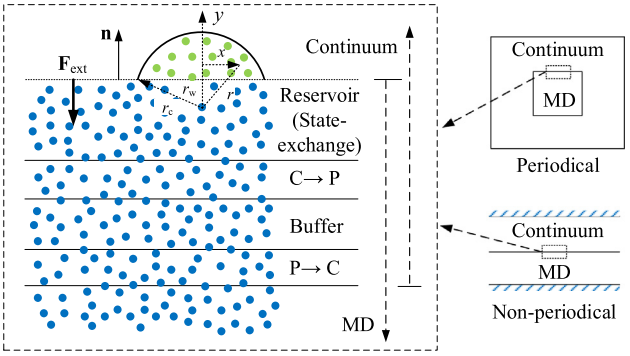

Fig. 4. Structure of the open coupling boundary for MD.

conditions. In order to efficiently deal with the open boundary conditions, special structure for the coupling boundary of MD is needed, which is sketched in Fig. 4. Generally the boundary consists of C → P region, P → C region, buffer region and a reservoir region (especially for state-exchange). The constraints for molecule motion (reconstruction operator) is applied to the C → P region, while the compression operator is applied to the P → C region to generate boundary condition for continuum method. Since the artificial effects are introduced in the coupling process, a buffer region is placed between the C → P and P → C regions to reduce the effects on the MD region that is concerned. Here we use boundary cells and controlled cells to denote the cells of MD simulation in reservoir region and C → P region correspondently.

For the state-exchange coupling, the C → P region is further covered by a molecule reservoir to provide molecule source and sink. As shown in Fig. 4, in a simplified condition when all the sides of the MD region are enclosed by continuum region, the reservoir region facilitates the utilization of periodical boundary condition for MD. Because the molecule motion in C → P region is controlled and the artificial effects are buffered, the molecule motion in reservoir will not influence the main MD region. However, if a single open boundary exists, the special treatments should be applied. A common idea is to exert an external force $\mathbf{F}_{ext}$ to the molecules in the outermost boundary cells of the reservoir to prevent the molecules moving out of the MD region, such as the forces proposed by O'Connell and Thompson [96] and Nie et al. [98]. Werder et al. [99] argued that the external force should exert the correct mean pressure of MD and minimize the local disturbance. Therefore, the external force is derived from the total forces between the considered molecule and the imagined molecules outside the computational domain based on the radial distribution function, as shown in Fig. 4.

However, the utilization of forces cannot prevent the molecules from moving out of the computational domain. Werder et al. [99] further proposed a reflection and insertion boundary scheme, in which the outermost boundaries of each boundary cell of MD are considered as specular walls moving with the macroscopic normal velocity of the cell. After each MD time step, the walls return to their initial position. The molecules outside the computational domain are then refilled into the vacancy of the inwards moving cells.

Inserting molecules into the boundary cells is also difficult especially when the fluid is dense and the inserted molecules tend to overlap with other molecules. A widely used method is the USHER algorithm proposed by Delgado-Buscalioni and Coveney [100]. The USHER is similar to Newton–Raphson iteration for finding an insertion position with a given energy U_0. The main modifications are using large displacement when the energy difference is large to remove the initial overlap, and limiting the maximum displacement in the later downhill processes. They also suggested to give up an initial search and start a new one when the uphill

movement occurs, in order to further increase the efficiency of the algorithm.

As for the flux-exchange coupling, the reservoir region is not necessary, and the molecules are directly inserted into the controlled cells according to the mass flux.

In the next two sections both the state-exchange and flux-exchange coupling methods are briefly reviewed.

4.1.2. State-exchange coupling

In the state-exchange coupling method, the macroscopic velocities and temperatures are exchanged between the MD and continuum methods. In this coupling the information transfer in P → C region is simple, one can use Eq. (8) to calculate velocities and temperatures as the Dirichlet boundary condition for continuum method. Li et al. [101] also proposed a thermodynamic field estimator (TFE) to directly generate continuous field distributions by maximize the total possibility of the molecule data when the fluid has local Maxwell distribution in the whole field.

On the other hand, the reconstruction process is more complex because the motion of all the molecules in the C → P region should be controlled by a small number of macroscopic values. There are mainly two types of methods to transfer the macroscopic values to the MD simulation, the *velocity reset* and *constraint dynamics*.

In the *velocity reset method*, the molecular velocities in the cell of C → P region are reset by Maxwell distributions with local fluid velocities and temperatures, which can be interpolated from the macroscopic simulation results [102]. A subtle model called optimal particle controller (OPC) is further proposed by Li et al. [103] to minimize the disturbance to the MD when resetting the molecular velocity. The concept is to match the targeted velocity distribution function by resetting the molecular velocities. They combined OPC and TFE with feedback control to generate an extended boundary condition.

As for the *constrained dynamics methods*, in the works of O'Connell and Thompson [96] and Wang et al. [104], the average velocity in the Jth boundary cell is relaxed to the prescribed macroscopic velocity $\mathbf{u}_J$ by adding relaxation term to the molecule motion Eq. (6):

$$\frac{d\mathbf{v}_i}{dt}=\frac{\mathbf{F}_i}{m}+\frac{\xi}{\Delta t_{\mathrm{MD}}}\left(\mathbf{u}_J-\frac{1}{N_J}\sum_{n=1}^{N_J}\mathbf{v}_n\right) \tag{22}$$

Here $\mathbf{v}_i$ is the molecule velocity in the cell, N_J is the molecule number in the cell and ξ is a relaxation parameter. O'Connell and Thompson [96] used $\xi = 0.01$ and Wang et al. [104] dynamically determined the ξ by summing Eq. (22) over the cell and solving a local ξ. Nie et al. [98,105] pointed out that the constraint should satisfy the relation $\sum_n \dot{\mathbf{v}}_n/N_J = D\mathbf{u}_J/Dt$, so they proposed a constraint scheme as:

$$\frac{d\mathbf{v}_i}{dt}=\frac{\mathbf{F}_i}{m}-\frac{1}{mN_J}\sum_{n=1}^{N_J}\mathbf{F}_n-\frac{1}{\Delta t_{\mathrm{MD}}}\left(\frac{1}{N_J}\sum_{n=1}^{N_J}\mathbf{v}_n-\mathbf{u}_J(t+\Delta t_{\mathrm{MD}})\right) \tag{23}$$

Some further modifications of Eq. (23) were proposed. For example, Yen et al. [106] used the temporal average values in M successive MD time steps to substitute the $\sum_n \mathbf{F}_n$ and $\sum_n \mathbf{v}_n$ to eliminate the thermal fluctuation. Sun et al. [107,108] suggested to use interpolated local macroscopic velocity in Eq. (23).

The above works mainly considered the velocity or momentum exchange. The temperature exchange can be also manipulated by velocity reset or constrained motion. For example, Liu et al. [109] rescaled the molecular velocity according to the temperature of continuum method $T_{J,\mathrm{C}}$ by

$$\mathbf{v}_i^*-\mathbf{u}_J=\sqrt{T_{J,\mathrm{C}}/T_{J,\mathrm{MD}}}\left(\mathbf{v}_i-\mathbf{u}_J\right) \tag{24}$$

in which $T_{J,\mathrm{MD}}$ is the MD temperature in the cell before rescale, and $\mathbf{v}_i^*$ is the rescaled velocity. Sun et al. [107,110] suggested to use the Langevin equation to constrain the temperature:

$$\frac{d^2y_i}{dt^2}=-\alpha\frac{dy_i}{dt}+\frac{\mathbf{F}_i}{m}+\frac{\mathbf{F}_{\mathrm{rand}}}{m} \tag{25}$$

in which α is a damper constant and $\mathbf{F}_{\mathrm{rand}}$ is a random force vector generated from Gaussian distribution with vanished mean value and the standard deviation related to the temperature.

4.1.3. Flux-exchange coupling

Besides the state-exchange coupling scheme, the coupling can be also through flux-exchange. Flekkoy et al. [111] proposed the first flux-exchange scheme for mass and momentum fluxes. The mass flux $\rho\mathbf{u}\cdot\mathbf{n}$ and momentum flux $(\rho\mathbf{uu}+\mathbf{\Pi})\cdot\mathbf{n}$ for MD can be calculated from Eq. (8) and applied as boundary conditions to continuum models. For the inverse information transfer, assuming $s(\mathbf{x}, t)$ is the rate of the number of molecules that move out of a boundary cell through MD boundary with cross section A, then the relations of mass and momentum fluxes are:

$$ms(\mathbf{x},t)=A\rho\mathbf{u}\cdot\mathbf{n} \tag{26}$$

$$ms(\mathbf{x},t)\langle\mathbf{v}\rangle+\sum_i\mathbf{F}_{\mathrm{ext},i}=A(\mathbf{\Pi}+\rho\mathbf{uu})\cdot\mathbf{n} \tag{27}$$

It can be seen that Eq. (27) is satisfied if the average velocity of the inserted molecules $\langle\mathbf{v}\rangle$ is equal to $\mathbf{u}$, and the overall force $\sum_i\mathbf{F}_{\mathrm{ext},i}$ equals the stress force $A\mathbf{\Pi}\cdot\mathbf{n}$. Thus, the molecules can be inserted by Maxwell distribution with mean velocity $\mathbf{u}$. Also, instead of applying uniform external forces to the controlled region, Flekkoy et al. [111] suggested to use a weight function $w(x)$ and distribute the force by $\mathbf{F}_{\mathrm{ext},i}=\left[w(\mathbf{x}_i)/\sum_i w(\mathbf{x}_i)\right]A\mathbf{\Pi}\cdot\mathbf{n}$.

The flux-exchange method is also extended to the energy flux [112–114]. The energy flux $\mathbf{E}$ can be calculated from MD with the following expression [115]:

$$\frac{1}{V_{\mathrm{CV}}}\left\langle\sum_{i=1}^{N}m\varepsilon_i\mathbf{v}_i+\frac{1}{2}\sum_{i=1}^{N}\sum_{j=1}^{N}\mathbf{r}_{ij}\mathbf{F}_{ij}\mathbf{v}_i\right\rangle_{\delta t}=\mathbf{E} \tag{28}$$

(Here the definition of $\mathbf{r}_{ij}$ is the negative value of the $\mathbf{r}_{ij}$ Refs. [113,114].) The ε_i is the energy of molecule i: $\varepsilon_i=mv_i^2/2+\sum_j\varphi(r_{ij})/2$ [24,115]. Then the energy flux can be used as the boundary condition for continuum method. For the boundary of MD, Delgado-Buscalioni and Coveney [113,114] used the following expression for energy flux balance:

$$ms\langle\varepsilon\rangle+\left\langle\sum_i\mathbf{F}_{\mathrm{ext},i}\cdot\mathbf{v}_i\right\rangle-\left\langle\mathbf{J}_{\mathrm{Q}}^{\mathrm{ext}}\right\rangle\cdot\mathbf{n}=A(\rho\mathbf{u}e+\mathbf{\Pi}\cdot\mathbf{u}+\mathbf{q})\cdot\mathbf{n} \tag{29}$$

The three terms on both the left and right hand sides of Eq. (29) are advection, dissipation and conduction terms, and each pair should be equal respectively. For the advection part the inserted energy for a molecule is $\varepsilon_i=v_i^2/2+\sum_j\varphi(r_{ij})/m$ and the average inserted energy $\langle\varepsilon\rangle$ should be equal to $e=u^2/2+3T/2+\phi$, in which ϕ is the internal energy due to molecule interaction. If the molecules are inserted with Maxwell distribution, we have $\langle v_i^2/2\rangle=u^2/2+3T/2$. Therefore, the average potential energy of the inserted molecule should be ϕ, and still the USHER methods [100] can be used to find proper positions of insertion. The dissipation term is satisfied if the weight function $w(x) = 1$ is used in the momentum coupling. As for the conduction term, the Fourier's law is assumed and a corresponding temperature gradient is generated in the controlled cells by thermostats.

4.1.4. Validations and applications

The coupling schemes are usually validated by the simulations of simple examples such as the steady and unsteady Couette or Poiseuille shear flows [96,98,103,104,106,111,112,114], flows in nano-channels [102,107], lid-driven flows in cavity [105]. As for the applications, the coupling methods are applied to problems such as the flow in nano-channels with boundary roughness [98,108,109], flow past carbon nanotubes [99], the condensation of gas flow in nano-channels [110], the impingement of a nano-droplet [116], the dynamic spreading of droplet [117], the contact-line problems [118,119] and the electroosmotic flows in micro-channel [120]. It can be seen that contrary to the extensive researches on the information exchange techniques between MD and continuum methods, the validations and applications of this hybrid atomistic-continuum method is limited. The reason is that in the domain decomposition framework the MD simulation also has a sub-region. Therefore, a complete separation of space scale is needed to reduce the MD simulation to a small region that is computational acceptable. However, taking the channel flow as an example, although the scale is separated along the radial direction and MD is only adopted near the boundary, there is no clear scale separation along the axial direction. Thus a simulation for long channel cannot be implemented under the framework of domain decomposition [121]. We will also discuss this limitation in Section 7.

4.2. Adaptive resolution scheme and the multiscale methods between MD and DPD/SDPD

As shown in Eq. (19), the motion equations of DPD and SDPD are similar to the motion equations of MD since all the equations have reversible interactive forces between particles, in spite of the dissipative and random forces of DPD/SDPD. Therefore, the techniques described in the previous section for the coupling methods of MD can be transplant to the coupling methods of DPD/SDPD. For example, Fedosov and Karniadakis coupled MD, DPD and continuous method, and the velocities were the information transferred among the methods [122]. For the MD and DPD, the tangential velocity is imposed by the relaxation method similar to the constrained motion. The normal velocity is applied by reflection and insertion [99]. They also found that the USHER algorithm [100] is not needed for DPD and the random insertion is enough.

However, the coupling between MD and DPD/SDPD through velocity can be regarded as an indirect coupling because the microscale and mesoscale are coupled through macroscopic variables. A direct coupling between microscale and mesoscale should be invented to take advantages of the particle features of DPD/SDPD. Then, the coupling through Adaptive Resolution Scheme (AdResS) is proposed. Since both MD and DPD/SDPD contain interactive forces between particles, a smooth transition of the interactive forces in a transition region would accomplish the coupling. In this section, the AdResS will be firstly introduced, and then its applications in the coupling simulations will be reviewed.

4.2.1. Adaptive resolution molecular-dynamics simulation

The molecular dynamics simulation itself can have different levels of resolution, such as using atomistically resolved molecules or treating the whole molecule as a spherical particle. The one-particle coarse-grained molecule is enough for the hydrodynamic behavior, but the flow boundary or reaction are sensitive to the structure of the molecule. The degrees of freedom and the computational intensities of the models are different, so proper models should be chosen for different applications. The AdResS is then proposed by Praprotnik et al. [123,124] to establish a MD with multiple resolutions of molecules, in which the molecules can switch between atomistic level and one-particle coarse-grained level on-the-fly. In AdResS an effective pair potential $U^{\mathrm{cm}}(r)$ is firstly constructed for the coarse-grained molecules based on the fully atomistic model. The center of mass radial distribution function and pressure of the two models should be matched. Then, the domain decomposition framework is employed and the two models with different degrees of freedoms are coupled through an interface layer, in which both descriptions of the molecules are adopted. In order to transform the molecules smoothly, the interactive force for the molecules inside the interface layer is the linear combination of the forces of fully atomistic model and coarse-grained model:

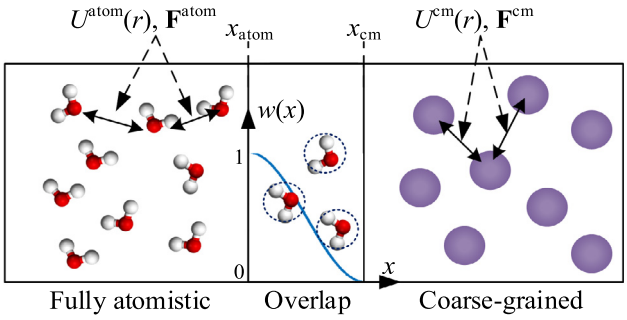

Fig. 5. Sketch of the Adaptive Resolution Scheme.

$$\mathbf{F}_{\alpha\beta} = w(R_\alpha)w(R_\beta)\mathbf{F}^{\mathrm{atom}}_{\alpha\beta} + \left[1 - w(R_\alpha)w(R_\beta)\right]\mathbf{F}^{\mathrm{cm}}_{\alpha\beta} \tag{30}$$

in which $\mathbf{F}_{\alpha\beta}$ is the effective interactive force between two molecules, $\mathbf{F}^{\mathrm{atom}}_{\alpha\beta}$ and $\mathbf{F}^{\mathrm{cm}}_{\alpha\beta}$ are the fully atomistic force and coarse-grained force between the two molecules. R_α and R_β are the positions of molecule's center of mass. The w is a weight function which is 0 in the coarse-grained region, 1 in the atomistic region and changes from 0 to 1 in the interface layer. A sketch of the coupling scheme is drawn in Fig. 5. The changing of the molecule's number of degrees of freedom can be regarded as a phase-transition, so thermostat should be used to deal with the latent heat when particle travelling between the two sub-regions and control the temperature of the system. The model has been used for tetrahedral molecule [123,124] and water molecules [125]. Based on an algorithm SWINGER to assemble, disassemble, and reassemble clusters, Zavadlav et al. [126] also coupled the fully-atomistic model with supramolecular MARTINI model for four-water clusters with AdResS. This method has been used to study the protein hydration processes [127].

4.2.2. Multiscale SDPD based on changing particle size

Besides the MD, the SDPD also has multiresolution schemes, and this scheme has been applied in the multiscale simulations. Therefore, a short discussion of the multiscale SDPD is provided here for completeness. It has been mentioned that the SDPD has a physical scale which is related to the volume of particle (parameter h in the weighting function). Kulkarni et al. [69] showed that when the particle size reaches molecular scale, the diffusion coefficient of SDPD can be matched with an all-atom L-J system, and the temperature, pressure and average density remain scale-invariant. Therefore, by changing the particle size, SDPD has the potential to represent scales from continuum scale to molecular scale. Based on this property of SDPD, a multiscale SDPD scheme is proposed within the domain decomposition framework [68,69]. The particles in different sub-regions have different particle sizes (masses) and number densities. Since the length scales in different sub-regions are different, the smoothing length h for each particle is changing on-the-fly, which is inversely related to the local number density by $h = h_0 n^{-1/3}$. The particles split or combine

according to the ratio between the particles sizes when passing the boundary between two sub-regions. This multiscale SDPD has been tested for both single-component shear flows [69] and multicomponent models [68].

4.2.3. Coupled MD-DPD/SDPD methods with AdResS

As exhibited in Section 4.1, one of the major difficulties for the coupling between MD and continuum methods is the difference between the descriptions from continuous fields and discrete particles. From this point of view, the particle-based DPD and SDPD method has the advantage to be compatible with MD. It can be seen that the conservative forces of DPD in Eq. (19) and the reversible deterministic forces of SDPD are similar to the interaction between molecules. Then, the particle interactions in DPD/SDPD can be regarded as another coarse-grained descriptions of large molecules. Therefore, the idea of AdResS can be used to smoothly shift the interaction forces between MD and DPD/SDPD.

Based on this idea, Petsev et al. [128] proposed a coupling scheme between MD and SDPD, in which forces in the overlapping region is a linear combination of MD forces and SDPD reversible forces:

$$\mathbf{F}_{\alpha\beta}^{\text{buffer}}\Big|_{\text{rev}} = w(z_\alpha)w(z_\beta)\mathbf{F}_{\alpha\beta}^{\text{MD}} + \left[1 - w(z_\alpha)w(z_\beta)\right]\mathbf{F}_{\alpha\beta}^{\text{SDPD}}\Big|_{\text{rev}} + \xi\mathbf{F}_{\alpha\beta}^{\text{th}} \tag{31}$$

The subscript "rev" represents the reversible part. The $\mathbf{F}_{\alpha\beta}^{\text{th}}$ is an additional thermodynamic force to suppress the density gradient in the overlapping region, and ξ is a weighting function to ensure that the thermodynamic force contributes maximally in the overlapping region. Similar to the AdResS, since the particles in two sub-regions can be regarded as two phases, thermostat should also be applied to maintain the temperature of the system. The SDPD particles have the same size as MD molecules in their work, and the multiscale SDPD is expected to further couple with a coarse SDPD region. Similarly, Zavadlav and Praprotnik [129] proposed a coupling scheme between MD and DPD for water molecules. Petsev et al. [130] combined the AdResS with multiscale SDPD to construct a coupling method between MD and SDPD for multicomponent problems. In their model, the AdResS is firstly used to transfer MD molecules into pure solvent or solute SDPD particles with molecular size. Then, the multiscale SDPD scheme is used to combine solvent or solute particles into particles with mass fractions in the more coarse SDPD models.

4.2.4. Coupled MD-continuum method with AdResS

The discussion of the coupling with MD in Section 4.1.1 mentioned that one of the difficulties is the insertion of molecules in to dense fluid. The situation is worse when the inserted molecules have complex structures. As described before, the multiresolution MD with AdResS provides a gradually conversion from fully atomistic molecules to coarse-grained molecules. Moreover, by adding thermodynamic forces to the hybrid region, the scheme can serve as molecule reservoir for μVT ensemble [131,132]. Thus AdResS can be a promising interfacial technique for the coupling between continuum models and complex molecules to simplify the molecule insertion. Delgado-Buscalioni et al. [133] combined the AdResS into their hybrid MD model, so that their flux coupling scheme can be applied to coarse-grained molecules in regardless of the real molecule structure, and the momentum flux can be transferred to the fully atomistic region through AdResS since this scheme conserves linear momentum. They also found that by putting the coupling boundary of CFD inside the fully atomistic region (which means the AdResS is entirely contained in the buffer region), the restrictions on the matching between coarse-grained models and atomistic models in AdResS can be loosen [134].

4.3. Coupling DSMC methods with other methods

4.3.1. Coupling scheme between DSMC and continuum methods

Since the aerothermodynamics of hypersonic re-entry vehicles can experience flows from continuum region to rarefied region, there is a long research history on the hybrid method between DSMC and continuum N-S solvers [135,136]. Some detailed review of the coupling scheme can be found in Refs. [137,138]. In this section we mainly focus on the common features of the coupling scheme in the framework of domain decomposition.

Since DSMC is a particle-based method similar to the MD, the coupling scheme between DSMC and continuum is quite similar to the MD-continuum coupling methods. Both the state-exchange and flux-exchange coupling can be used for the information exchange. Here again the compression operator is straightforward, while the reconstruction operator is the main problem. Since the velocity distribution function is important for the DSMC, a relation between distribution functions and the macroscopic variables is needed. The kinetic theory is a great help and the Chapman-Enskog expansions are used.

In an early work of Hash and Hassan [139], the Chapman-Enskog distribution function corresponding to the variable hard-sphere (VHS) model [27] is written as:

$$f = f^{\text{eq}}\left[1 - \frac{4\kappa\beta^2}{5nk}\left(\beta^2 C'^2 - \frac{5}{2}\right)C_i'\frac{\partial \ln T}{\partial x_i} - \frac{4\mu\beta^4}{\rho}\left(C_i'C_j' - \frac{C'^2}{3}\delta_{ij}\right)\frac{\partial u_i}{\partial x_j}\right] \tag{32}$$

Here f^{eq} is still the Maxwell distribution, $\beta^2 = 1/2RT$. The thermal conductivity κ and viscosity μ are corresponding to the VHS model. In their work there is no overlapping or hand-shaking region between continuum and DSMC sub-regions. For the flux-exchange scheme (Marshak condition), the net flux on the interface is set to the summation of the half-flux from DSMC side, which is by the summation of crossing particles, and the half-flux from continuum side, which is calculated from the Chapman-Enskog distribution function. For the state-exchange scheme, the interfacial values are interpolated from the two sub-regions. Couette flow test shows that the Marshak condition offers the better performance. Also, the Chapman-Enskog distribution function is superior to the equilibrium Maxwell distribution since the gradient effects are important, although some later blunted cone test cases show that the Maxwell distribution is sufficient for specific problems [140,141].

However, the direct flux-exchange can lead to large fluctuations when the number density of particle is small. In order to solve this problem, an overlapping region which includes a DSMC reservoir and a buffer region is added [142–145]. The sketch of the boundary region for DSMC is similar to the open boundary of MD in Fig. 4, but is without the continuum to particle (C → P) region for constrained motion. During the information transfer from continuum to DSMC region, the particle in reservoir region are regenerated with the macroscopic variables from continuum simulation based on Maxwell distribution when the flow is close to equilibrium [142–144] or Chapman-Enskog distribution when the flow is away from equilibrium [145]. The buffer region is used to decrease the artificial effects in the reservoir region and increase the quality of particles entering the DSMC region. As for the information transfer from DSMC to continuum model, Roveda et al. [142] used particles in the buffer region in addition to the boundary cells for the statistical calculation to suppress the noise of macroscopic values calculated from DSMC. The information preservation method and

sub-relaxation technique are also used to decrease the statistical scatter of the original DSMC [145–147]. The Schwarz alternative method can be used to decouple the time scales between DSMC and continuum method for the unsteady simulations [148]. The hybrid DSMC-continuum method has been used in many rarefied gas flow problems such as hypersonic flow over hollow-cylinder-flare geometry [149], blunt-body [150], rarefied supersonic gas flows in micro-nozzles [151].

A special feature in the coupling between DSMC and continuum method is a criterion for the position of interface. As mentioned in Section 2.3.1, the *Kn* number determines the rarefaction of gases and the flow region, so it can be the criterion to determine where the continuum breakdown happens and the DSMC should be used. Several breakdown parameters related to *Kn* are proposed [145], and the commonly used parameters are the Bird's parameter $P = \frac{U}{\rho v}\left|\frac{d\rho}{ds}\right|$ [152], the Gradient-Length Local (GLL) Knudsen number $(Kn)_{\mathrm{GLL}} = \frac{\lambda}{Q}\left|\frac{dQ}{dl}\right|$ [153,154] and the breakdown parameter for Chapman-Enskog distribution $B = \max\left\{\left|\tau_{ij}^{*}\right|, \left|q_i^{*}\right|\right\}$, $\tau_{ij}^{*} = \frac{\mu}{p}\tau_{ij}$, $q_i^{*} = \frac{1}{p}\left(\frac{2m}{kT}\right)^{1/2} q_i$ [155,156]. Here U is velocity, v is collision frequency, λ is mean free path, Q is a variable of interest such as density, temperature and pressure, s is distance along the streamline and l is a length of the simulation. The τ_{ij} and q_i are components of stress tensor and heat flux given by Eqs. (4) and (5). The $P > 0.05$, $(Kn)_{\mathrm{GLL}} > 0.05$ are commonly used thresholds for the continuum breakdown. The threshold for B is not clear. Garcia et al. [156] suggested B over 0.02 while Sun et al. [145] suggested B over 0.002 for their simulations of flows over a flat plate. These criteria facilitates the utilization of adaptive mesh [142,145] and algorithmic refinement scheme [156,157], in which the DSMC sub-region changes during the simulation according to the calculation results.

4.3.2. Coupling scheme between DSMC and MD

The researches on the coupled MD-continuum and DSMC-continuum methods promote the further researches on the coupling between MD and DSMC. The MD can be used in the region near solid boundary. Also, the particle feature of DSMC facilitates the information exchange between MD and DSMC.

When the particles in DSMC and MD have one-on-one mapping, the DSMC can be regarded as a special MD scheme with statistical sampling of the collisions. For example, Nedea et al. [158] proposed a coupled MD-DSMC method in which an extended DSMC is used for dense flows. The MD-to-DSMC information transfer is achieved by simply copying particle positions and velocities of MD into the reservoir of DSMC. The inverse transfer is more difficult because the particles in DSMC can overlap each other and generate large force and temperature jump in the interface. Therefore, they chose to transfer macroscopic temperature and velocities to MD by the state-exchange methods similarly to the coupling between MD and continuum, which is described in Section 4.1.2. Gu et al. [159] proposed a similar method, in which the particles that leave the DSMC or MD region will be initially deposited in a free-flight zone before entering the other region.

However, in the above couplings the particles of DSMC has a one-on-one mapping with the particles in MD. This mapping degrades the advantage of DSMC, in which a particle can represent a cluster of molecules and reduce the calculation costs. In order to prevent this disadvantage, Liang and Ye [160] exchanged the information between DSMC and MD based on the velocity distribution. In their model the velocity distribution functions of the particles that leave DSMC region or MD region through the coupling boundaries are extracted and used in the insertion of particles. Watvisave et al. [161] employed the similar method based on velocity samplings to couple DSMC with MD, in which MD is used near the solid boundary to deal with the gas–surface interactions.

4.4. Coupling LBM with other methods

4.4.1. Coupling scheme between LBM and continuum methods

As mentioned in Section 2.3.3, the LBM is an efficient method for the simulation with complex boundary conditions, but for the flow and heat transfer in regular geometries, the macroscopic continuum methods are preferred. Therefore, attentions are paid to the hybrid scheme between LBM and continuum methods. A comprehensive review about the theory and applications of coupling between LBM and continuum was given in our previous work [162], and the main ideas are summarized in this section.

All the existing domain decomposition hybrid LBM-continuum methods are based on the state-exchange with overlapping regions. The compression operator for the boundary condition of continuum methods is naturally offered by the moments of distribution functions as Eq. (17). As for the reconstruction operator, the Chapman-Enskog expansions Eq. (12) can be adopted to the discrete distribution functions of LBM and link the distribution functions to macroscopic variables. Therefore, it provides a method to build the reconstruction operator. By expending the spatial and temporal derivatives and the evolution equation (15) into different orders of ε, one can derive the expressions for $f_i^{(1)}$ and $f_i^{(2)}$. Then the first and second order approximations of f_i can be obtained by adding $f_i^{(1)}$ and $f_i^{(2)}$ into f_i^{eq}:

$$f_i^{O(\varepsilon)} \approx f_i^{\mathrm{eq}} - \tau\Delta t D_i f_i^{\mathrm{eq}} \tag{33}$$

$$f_i^{O(\varepsilon^2)} \approx f_i^{\mathrm{eq}} - \tau\Delta t D_i f_i^{\mathrm{eq}} + \Delta t^2 \tau\left(\tau - \frac{1}{2}\right) D_i^2 f_i^{\mathrm{eq}} \tag{34}$$

It should be mentioned that the above derivations are not limited to the LBGK model, it can be extended to other LBM models such as the convection–diffusion model and multiple-relaxation-time-LBM (MRT-LBM) [163].

Since the expression of the first order approximation is simpler, it is widely adopted in the existing works. In most of the researches Eq. (33) is not directly used, but the specific LBM models are mixed into the derivations. In the early works, Albuquerque et al. [164] and Van Leemput et al. [165,166] proposed coupled LBM and finite difference methods for 2D and 1D diffusions. The equilibrium distribution and first order expansions have the forms [164]:

$$f_i^{\mathrm{eq}} = \frac{\rho}{2d},\ f_i^{(1)} = -\frac{\tau\Delta t}{2d}\mathbf{c}_i \cdot \nabla\rho \tag{35}$$

Luan et al. [167] proposed the reconstruction operator for the LBGK model:

$$f_i = f_i^{\mathrm{eq}}\left[1 - \frac{\Delta t\tau U_{i\beta}}{c_s^2}\left(U_{i\alpha}\frac{\partial u_\beta}{\partial x_\alpha} + \nu\nabla^2 u_\beta + \frac{\nu S_{\alpha\beta}}{\rho}\frac{\partial\rho}{\partial x_\alpha}\right)\right] \tag{36}$$

in which $U_{i\beta} = c_{i\beta} - u_\beta$ and $S_{\alpha\beta} = \partial u_\beta/\partial x_\alpha + \partial u_\alpha/\partial x_\beta$. Benchmark simulations including the flow over backward-facing step, flow around a circular cylinder and lid-driven cavity flow were used to validate the coupling scheme. They also used the coupling scheme to simulate the flow around the NACA0012 airfoil and porous medium [168]. Results showed that the coupling method has better efficiency than the multi-block LBM. Xu et al. [169] further examined the reconstruction operator and showed that it has good precision. The coupling scheme is also expended to the simulation of convection-diffusion problems based on the double-distribution-function LBM [170–172].

The reconstruction operators in the above researches are derived for specific LBM models, so the procedures are lack of generality. Tong and He [173] applied Eq. (33) as the generalized reconstruction operator and showed that most of the reconstruction operators in the existing works can be derived from Eq. (33). Based on this generalized operator, they proposed the coupling

scheme for incompressible LBM and unsteady coupling simulations.

Although the reconstruction operators with first order approximation are widely adopted in the researches, the second order approximation is also considered in some works. For example, Salimi and Taeibi-Rahni [174] derived the reconstruction operators for D2Q9 and D3Q19 MRT-LBM models, and in their works the second order approximation was considered. Van Leemput et al. [165,166] also discussed the influence of the second order terms on the accuracy of the reconstruction operator, and they found that the second order operator can assure a global second order error behavior. As mentioned before, one would expect the operators have the property $\mathcal{QR} = \mathcal{I}$. Therefore, the approximations of f_i should recover the same density and velocity as shown in Eq. (17). A detailed analysis for the orders of reconstruction operator were given by Tong et al. [163] in a recent work. They showed that the first order approximation can recover density but cannot correctly recover the velocity or momentum. An error related to the gradient of deviatoric stress tensor occurs in the momentum because of the neglect of the second order derivatives. On the contrary, second order models can recover both density and momentum. Based on an early study of Skordos [175], Tong et al. [163] also added a correction term to the first order operators to correct the error. They found that the modified first order operators has the same accuracy as second order operators, so they suggested to use modified first order operators in the future coupling simulations.

The coupled LBM and continuum methods have been used in some applications and show better performance than pure LBM or continuum methods. For example, Chen et al. [176] used the coupled method to simulate the mass transfer and chemical reaction in the gas channel (by FVM), porous gas diffusion layer and catalyst layer (by LBM) of a proton exchange membrane fuel cell (PEMFC). Velivelli and Bryden [58,59] combined LBM into the traditional methods in the region where LBM's space and time steps are more efficient than the traditional methods to improve the computational efficiency. Salimi et al. [177,178] used the coupled MRT-LBM and FVM to simulate the unsteady fluid flow passing over a porously covered square cylinder. The porous region were either simulated by LBM in representative elementary volume scale [177] or pore-scale [178] because the time steps were small there. Tong et al. [179] also employed the coupled MRT-LBM with FVM to simulate the fouling process on tubes, in which the fouling layer on the tubes grew during the particle deposition and the boundary condition for the flow was changed. The MRT-LBM was used in the region near tubes to deal with the changing boundary. The particle motion was simulated by a probabilistic cellular automata model, and the energy, force and momentum analyses were used as criteria for particle collision, deposition and removal. The evolution of the shape of fouling layer was obtained.

The above applications demonstrate the conditions under which the LBM should be selected. The explicit nature of LBM gives it the advantage of high efficiency for unsteady simulations comparing with the traditional methods with same time steps, but also limits its size of time step. Therefore, the LBM should be used in the region where the characteristic time scale is compatible with the time step of LBM, and the implicit continuum methods should be adopted in the region where a longer time step can be adopted.

4.4.2. Coupling scheme between LBM and MD

Comparing with the domain decomposition multiscale hybrid scheme between other numerical methods, the coupling between LBM and MD receives less attention in the current researches. The main reason can be that the LBM is often regarded as an alternative to macroscopic method in the current researches. Therefore, it seems there are no new things in the coupling between LBM and MD. The coupling scheme of MD-continuum and LBM-continuum can be transplanted to the coupling between LBM and MD. For example, the boundary conditions for MD described in Section 4.1 can be used to transfer velocity information from LBM to MD [180–185], while the reconstruction operator can be used to generate the boundary condition for LBM from the velocity calculated in MD [185].

In the above coupling schemes, the information that exchanged between LBM and MD is only velocity. However, it can be seen that both the LBM and MD contain more information such as the stress tensor. Therefore, a straightforward thinking is to utilize more information. Recently, Tong et al. [186] realized that the relation between continuous velocity distribution function of MD and discrete distribution function of LBM can be used as the bridge for the coupling. Based on the construction procedure from Boltzmann equation to LBM [51], the similar Hermite expansion was firstly adopted to get the continuous distribution function for MD:

$$f(\mathbf{c}) = \omega(\mathbf{c})\rho\left[1 + \frac{\mathbf{u}\cdot\mathbf{c}}{c_s^2} + \frac{(\mathbf{u}\cdot\mathbf{c})^2}{2c_s^4} - \frac{u^2}{2c_s^2} + \frac{\boldsymbol{\Pi}_{\mathrm{id}} : \mathbf{cc}}{2\rho c_s^4} - \frac{c^2}{2c_s^2} - \frac{D}{2}(T-1)\right] \tag{37}$$

Here $\omega(\mathbf{c}) = \exp(-c^2/2c_s^2)/(2\pi c_s^2)^{D/2}$ and D is the dimension. The $\boldsymbol{\Pi}_{\mathrm{id}}$ represents the ideal part of the stress tensor of MD, which is the first term in the bracket of the expression for $\boldsymbol{\Pi}$ in Eq. (8). The molecule velocity in the boundary cells can be reset based on this velocity distribution. Then the Gauss-Hermite quadrature procedure was used to derive the expression for the discrete function of LBM as

$$f_i = \frac{w_i}{\omega(\mathbf{c}_i)} f(\mathbf{c}_i) = w_i\rho\left[1 + \frac{\mathbf{u}\cdot\mathbf{c}_i}{c_s^2} + \frac{(\mathbf{u}\cdot\mathbf{c}_i)^2}{2c_s^4} - \frac{u^2}{2c_s^2} - \frac{\tau\boldsymbol{\tau} : \mathbf{c}_i\mathbf{c}_i}{(2\tau-1)\rho c_s^4}\right] \tag{38}$$

One of the major problems between the coupling between LBM and MD is that the EOSs are different for the two methods. The EOS of LBM is an ideal gas model and the EOS of MD contains the non-ideal part related to the particle interactive force. Therefore, Tong et al. [186] chose to transfer the deviatoric stress tensor between the two method, and each method used its own pressure and EOS. Also, the non-ideal part of MD's stress tensor was determined by the extrapolation of previous coupling steps. The numerical simulation showed that the coupling based on distribution functions can transfer stress better than the velocity relaxation or velocity resetting with Maxwell distribution.

It can be seen that the coupling through distribution functions has a mesoscopic theoretical basis and generates a direct relation between the mesoscale and the microscale, so it is more fundamental than the phenomenal coupling through velocity. It also has the potential to be extended to higher-order LBM models. However, more questions emerge in this coupling scheme [186]. Firstly the inconsistency between EOSs of the two methods should be further considered because for the microscale flows the fluids can become compressible due to viscous effects [20]. The non-ideal LBM model should be considered in the future [187]. Secondly, the inclusion of higher order moments in the distribution functions increases the demanding for number of samplings and the statistical errors for the stress can be much larger than the velocity [188]. Therefore, better estimation methods for the higher order moments are also needed.

4.4.3. Coupling scheme between LBM and DSMC

The coupling through Hermite expansions is not limited to LBM-MD, in the earlier works, Di Staso et al. [189–191] proposed the coupling scheme between LBM and DSMC based on the Hermite expansions. For the information transfer from DSMC to

Table 1
The information exchange schemes between different numerical methods for domain decomposition multiscale simulations that are reviewed in the this work*.

	Continuum	MD	DSMC	LBM	DPD/SDPD
Continuum	——————**	Velocity reset, Constraint motion, Flux coupling	Maxwell or Chapman-Enskog velocity distribution function	Reconstruction operators based on Chapman-Enskog expansions	——————**
MD	Diriclet/Neuman boundary condition	AdResS with force transition†	Direct particle transfer, Velocity distribution function	Through continuum to LBM‡, Hermite polynomials	AdResS with force transition
DSMC	Diriclet/Neuman boundary condition	Through continuum to MD‡, Direct particle transfer, Velocity distribution function	——————**	Hermite polynomials	——————**
LBM	Diriclet/Neuman boundary condition	Through continuum to MD‡, Hermite polynomials	Hermite polynomials	——————**	——————**
DPD/SDPD	——————**	AdResS with force transition	——————**	——————**	AdResS with force transition†

* The direction of information transfer in the table is from methods in the left column to methods in the first row.
** The area with dashed lines are not in the scope of present review.
† Multiresolution MD/SDPD.
‡ The macroscopic values are firstly calculated, and then the information transfer methods from continuum to LBM or MD are employed.

LBM, the coefficients in the truncated Hermite expansions are calculated from the DSMC simulations and the continuous distributions are obtained. Then the discrete distribution functions of LBM are calculated by Gauss-Hermite quadrature similar to Eq. (38). For the inverse information transfer, the Hermite expansions are generated from LBM, and the particles in the reservoir region of DSMC are regenerated based on the distribution function. This procedure is similar as that described in Section 4.3.1. This coupling is more proper than the coupling between LBM and MD because the gas in both LBM and DSMC can be regarded as ideal gas.

4.5. Brief summary

In the above sections, the domain decomposition multiscale methods based on the numerical methods mentioned in Section 2 have been reviewed. The information exchange schemes between numerical methods are summarized in Table 1. It can be seen that the special feature of mesoscopic methods can facilitate the coupling. The particle interaction and evolution of DPD/SDPD are similar to the MD, so they can be coupled through a smooth transition of force schemes. The gas kinetic backgrounds of DSMC and LBM suggest the information transfer to the two methods through velocity distribution functions. Also, the particle feature of DSMC facilitates the direct particle transfer from MD to DSMC when the particles in the two methods have a one-on-one mapping. Detailed discussions will be given in Section 7.

5. Hierarchical multiscale methods

In the previous section the multiscale method based on domain decomposition are reviewed. As shown in the framework, the other kind of multiscale method is the hierarchical multiscale method, which includes serial, embedded and equation-free methods. Therefore, in this section we will briefly review these multiscale methods.

5.1. Serial

As a multiscale numerical method with one-way information transfer, the numerical scheme of serial method is simpler than the other methods. For the aspect of numerical simulation, usually the closure forms of governing equations, constitutive laws and boundary conditions are already given, and the microscopic numerical methods are conducted separately to obtain the parameters for the models. For example, mesoscopic method can be used for the calculation of permeability for the macroscopic simulations of porous flow [192]. MD is used to determine the contact angle, surface tension and other interfacial parameters that can be further adopted in the multiphase LBM [193–195]. Mortazavi et al. [196,197] used MD to calculate the interfacial thermal conductance between materials, which was used in the mesoscopic FE simulation in a representative volume element for the effective thermal conductivity of the composite. The effective thermal conductivity was further used in studying the performance of phase-change-material for the thermal management of Li-ion batteries.

Since the serial methods are based on the macroscopic models which are relatively more developed and closer to the practical applications than the mesoscopic and microscopic methods, the serial methods have been employed in many multiscale studies. Here we discuss the simulation of flow in nanotubes and contact line problems to show the difference between serial methods and the other methods.

Holland et al. [198] employed MD pre-simulations for the simulations of flows in nanotubes. The dynamic viscosity and pressure are assumed to be polynomial functions of density. For the boundary condition the Navier slip condition $u_{\text{slip}} = \xi\dot{\gamma}$ is used. The slip length ξ is a function of density and shear rate $\dot{\gamma}$ as $\xi = (c_1\rho + c_2)/\sqrt{1 - \dot{\gamma}/\dot{\gamma}_c}$, in which $\dot{\gamma}_c$ is critical shear rate. Since the solid molecular boundary is not smooth in microscale, a proper definition of the boundary position δ (distance to the center of surface wall atom) is needed, and it is also assumed to be a function of density. The Poiseuille flows are simulate by MD to extract the parameters in the polynomial fluid properties and boundary conditions. Then the above fluid properties and boundary conditions are used in the CFD simulations for nano-channel flows, which show good consistency with the full atomistic simulations.

Zhang et al. [199] also used the serial method to study the spreading of a nano-droplet on solid surface. The volume of fluid (VOF) method is adopted to simulate the behavior of the droplet, while the boundary conditions on the liquid-solid boundary and three-phase contact line are given by MD pre-simulations. For the three-phase contact line, a model based on molecular kinetic theory (MKT) is adopted, which relates the dynamic contact angle to the three-phase contact line slip velocity. Full MD simulations of dynamic droplet spreading are used to get the parameters in the MKT model. Meanwhile, a separate Couette flow is used to determine the slip length for the Navier slip model. The VOF simulations are consistent with MD simulations when using the slip velocity model and MKT model.

The similar nano-flows and contact line problems are also studied in the framework of domain decomposition, in which the MD is used in the boundary region to deal with the phenomena near the

boundary, and the continuum methods are employed in the bulk region to save the computation costs. For the serial multiscale method, the closure forms of the constitutive law and boundary condition are already known, such as the Newton's law of viscosity, the relations between slip length, density and shear rate, the MKT model for dynamic contact angle and contact line velocity. Then, a small number of MD pre-simulation can be used to determine the parameters of the relations. Since the MD is not needed to be manipulated on-the-fly, the cost of microscopic computation is greatly reduced.

It should be mentioned that the simplicity of serial multiscale method is based on the establishments of the closure relations, which can be very complex works in many situations. As mentioned before, if the closure relations are too complex to be applied or cannot be obtained, the embedded multiscale methods are suggested.

5.2. Embedded

The embedded multiscale method can be exemplified by the HMM proposed by E. et al. [72,73]. This method can be regarded as a point-wise coupling strategy, in which the microscale simulation is used to obtain the missing data in the grid points or control volumes of the macroscopic mesh-based methods. As mentioned in Section 3, the HMM contains an overall macroscopic model and a microscopic model. The compression operator and reconstruction operator are used to transfer information between the two models. There are two major issues for the HMM. The first is to properly apply constraints or boundary conditions to the microscopic simulations, which are usually determined by the specific microscopic model that is used. The second is to reduce the complexity of the microscopic simulation in the compression procedure, and this can be achieved by taking advantages of the separation of space and time scales.

Based on the characteristics of the embedded multiscale problems and methods, we divided the embedded methods into two categories: the *analytical embedded* and *numerical embedded*.

The *analytical embedded method* is typically called asymptotic analysis or methods of homogenization [21,200–202]. The problems considered in this kind of method are still described by macroscopic governing equations, but the parameters in the equations have small scale fluctuations due to the characteristics of the problems. Typical examples are the heat conduction in composite materials and the flow in porous media. The governing equations described the heat transfer and fluid flow in "microscopic" composite structures or pore-scale structures, but the phenomena that are concerned are in "macroscopic" averaged scale. The basic idea in the methods of homogenization is to expand the considered variables such as temperature and velocity into the macroscopic averaged variables and microscopic fluctuation variables. By the multiscale analyses of the governing equation, a homogenized equation for the macroscopic averaged variable and a cell problem in the representative elementary volume for the microscopic fluctuation variables can be derived. The analyses also provide the analytical relations between the results of cell problems and the homogenized parameters in macroscopic equations, such as effective heat conductivity and effective permeability. This kind of method is a specific research field and the cited monographs are suggested for more details.

In the *numerical embedded method* the processes in different scale are usually described by the governing equations or numerical methods in different scales. Therefore different scales are coupled from the numerical level but not the analytical connection. A typical example is the embedded method in which the microscale is described by atomistic methods. For example, Ren and E [74] used the HMM to simulate the flow of complex fluids and flows in microscale. The continuum method is still used to solve the macroscopic governing Eqs. (1) and (2), but the stress tensor $\mathbf{\Pi}$ or flow boundary conditions are given by MD simulations. The compression operators are straightforward and the sampling processes Eq. (8) can be applied to calculate $\mathbf{\Pi}$ and $\mathbf{u}$ from the MD results. The reconstruction operator relays on how to apply the macroscopic results as constraints to the MD. For the calculation of stress tensor in the inner region, the MD is constrained by the local strain rate. The Lees-Edwards periodic boundary condition can be used [203], in which the assumed replica systems are sliding above and below the simulation system. Ren and E [74] extended the idea by changing the shape of the simulation box according to the strain rates, and modifying the molecular velocity when a molecule moves out of a boundary and reenters from the opposite boundary. For the flow near boundary region, the boundary scheme similar as the velocity reset method described in Section 4.1.2 was applied. The pressure-driven flow for dumb-bell fluids, the driven cavity flows and the contact-line problems were simulated by the proposed HMM to validate the model, and the results showed good consistency with pure MD simulations.

Here the differences among decomposition, embedded and serial schemes can be shown in Fig. 6 for the micro-channel flow simulations. The domain decomposition applies MD to the boundary region while continuum methods in the inner region. The embedded and serial computations applied continuum methods in the whole region and use MD simulations to provide the missing information. The embedded method uses MD concurrently with continuum method, but the serial computation uses pre-calculations to determine the constitutive relations and boundary conditions for continuum simulations.

Some modifications and applications of the embedded MD-continuum method have also been proposed for the multiscale flow simulations. For example, De et al. [204] used the similar methods to simulate the polymeric fluid under one-dimensional

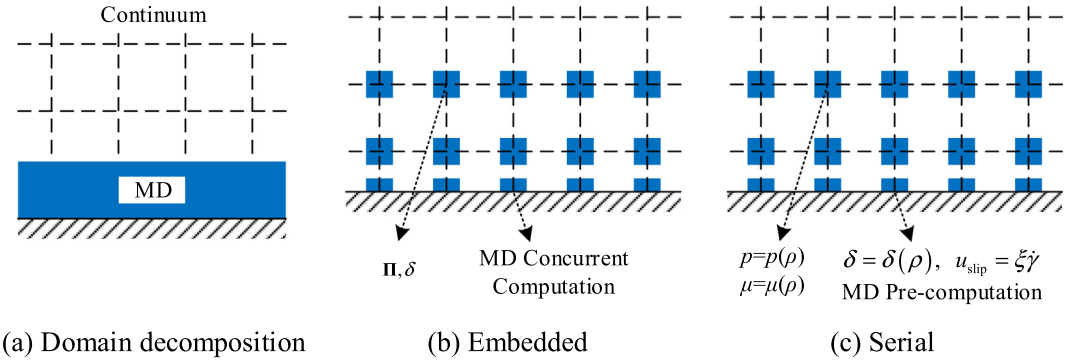

Fig. 6. Comparison of the simulations of flow in micro-channel by domain decomposition, embedded and serial schemes.

shear flow. Asproulis et al. [205] used the Parrinello-Rahman method [206] with deformation box to apply the strain rate constraint. Alexiadis et al. [207] used framed box instead of the deformation one for the embedded simulations. The MD cells were composed of buffer region, constrained region and main region similar to Section 4.1.2. The velocity and temperature reset schemes were applied to the constrained region. Meanwhile, in their work the temperature and momentum equations were reshaped into the Laplacian forms by assuming the constitutive laws are Eqs. (4) and (5) with deviation terms. Instead of using MD to provide the stress tensor, the MD simulations were used to directly calculate the Laplacians of the velocity and temperature. The method was further extended to multicomponent transfer problems [208]. Yasuda and Yamamoto used the HMM to simulate the shear flow of polymer melt between two plats [209]. In another work, they transformed the strain rate into a form that is convenient for MD and the diagonal elements all vanish [210]. They also transferred deviatoric stress tensor instead of the whole stress tensor from MD to the continuum simulations. Later, Murashima et al. [211] considered the more complex constitutive relations for viscoelastic polymer melt, in which the stress is influenced by the history of shear rate along the streamlines instead of the instantaneous local shear rate. Since the common Eulerian methods are hard to be used to trace the history along streamline, the Lagrangian SPH method was adopted. Then the history of the shear rate can be traced along with the Lagrangian particles. The stress tensor for the SPH was provided by the microscopic coarse-grained simulations. The two dimensional polymeric flow past a cylinder was used to show the application of the multiscale model. The thermal effects were also taken into consideration in further work [212].

Similar to the embedded concept, Borg et al. [213] proposed a field-wise coupling method. The procedure of the calculation is the same, which consists of macroscale solution, projection/reconstruction, constrained microscale solution and compression. In their model the MD simulations are used to provide the difference term between the deviatoric stress tensor of molecular fluids and that from Newton's law of viscosity. Different from HMM, the molecular simulation elements do not need to be collocated with the nodes of continuum simulations. Therefore, the polynomial fits should be used in the projection and compression steps for the information transfer. The MD simulation was constrained by adding artificial body force to the constrained regions. The method was validated by the simulations of one-dimensional Poiseuille flows with both Newtonian and non-Newtonian fluids. However, the method has difficulties to be extended to 2D and 3D applications, such as the preservation of continuity and the implementation of strain rate constrains to the MD simulations.

Borg et al. [121,214] also proposed a hybrid molecular-continuum method for one-dimensional incompressible flow in nano-channels, which is called internal-flow multiscale method (IMM). The MD sub-domains are small segments of the channel located along the flow direction. In each MD sub-domain the momentum balance with pressure gradient correction is employed. By applying a pressure gradient, the mass flow rate in each MD sub-domain can be obtained from the MD simulations. Then, the modeling procedure is to tune the pressure gradient in each sub-domain under the constraint of total pressure difference, and therefore equal the mass flow rate in each sub-domain to satisfy the mass conservation. The method has been extended to unsteady compressible flows [215]. When the DSMC is the microscopic solver, the IMM can be also extended to the compressible rarefied gas flow in nano-channels [216]. The method is further used in the water flows through carbon nanotube membranes [217,218].

The numerical embedded method is also used for the simulations of mass transfer in porous media, in which the pore scale simulations are conducted to provide the effective coefficients for the macroscopic transport equations. As for the reconstruction operator, Yue and E [219] considered the periodic, Dirichlet and Neumann boundary conditions of the microscopic cell problems based on the constraints of macroscopic gradients. They found all the boundary conditions show good convergence. Carr et al. [220] further coupled the thermal transport into the simulation and built a multiscale model to simulate the drying of wet porous media. In their models the fluxes were provided by the microscopic simulations to the macroscopic models instead of the transport coefficients [220,221].

For more complex applications, Lorenz and Hoekstra [222] used the HMM concept to build a multiscale model for suspension flow. The microscopic fully-resolved particle flow was constrained by the shear rates and particle volume fractions from macroscopic LBM simulation of flow and Lagrangian simulation of particles. The apparent viscosity of the flow and shear-induced diffusivities of the particles for these macroscopic models were then provided by the fully-resolved particle simulations.

5.3. Equation-free method

As mentioned in Section 3, the "Equation-Free" Multiscale Method was proposed by Kevrekidis et al. [77,78] to simulate macroscopic processes directly from microscopic methods without the close forms of macroscopic descriptions. The EFM is established step by step, from coarse time stepper and coarse projective integration for time evolution, to gap-tooth scheme for spatial extrapolation, and finally to the patch dynamics. In their work the compression and reconstruction operators are usually called restriction and lifting operators.

In the coarse time stepper, the macroscopic variables evolves for a microscopic time step δt based on the microscopic model. The procedure consists of lifting, microscale simulation and restriction steps. Then, the Using the Eqs. (20) and (21), the coarse time stepper can be expressed as:

$$\begin{aligned} &(1)\ u(\mathbf{x},t), d(\mathbf{x},t) \leftarrow \mathcal{R}[U(\mathbf{X},t)] \\ &(2)\ u(\mathbf{x},t+\delta t) = u(\mathbf{x},t) + \delta t f[u(\mathbf{x},t); d(\mathbf{x},t)] \\ &(3)\ U(\mathbf{X},t+\delta t) \leftarrow \mathcal{C}[u(\mathbf{x},t+\delta t)] \end{aligned} \tag{39}$$

In practice more complex schemes can be used instead of the forward Euler scheme in step (2). We will still use this forward Euler expression in the following discussions.

Then the coarse projective integration projects the macroscopic evolution in δt to the larger macroscopic time step Δt. The microscopic model should evolve for $k\delta t$, which is larger than the relaxation time τ_ε, so that the effects of the initial artificial higher-order moments can be eliminated. The changing rate of macroscopic variables is approximated by:

$$F[U(\mathbf{X},t)] \approx [U(\mathbf{X},t+k\delta t) - U(\mathbf{X},t)]/(k\delta t) \tag{40}$$

The temporal extrapolation is then adopted in the coarse projective integration for the macroscopic evolution:

$$U(\mathbf{X},t+\Delta t) = U(\mathbf{X},t+k\delta t) + (\Delta t - k\delta t)F[U(\mathbf{X},t)] \tag{41}$$

The higher-order extrapolations can be also used instead of Eq. (41).

As for the scale separation in space, the gap-tooth scheme is proposed [223]. In the gap-tooth scheme the space is divided into control volumes located at x_i, which is the same as general macroscopic numerical methods. Then the known microscopic models are applied in in small spatial intervals $[x_i - h/2, x_i + h/2]$. The h is much smaller than the length of macroscale control volume, and

large enough for the microscopic models to eliminate the artificial effects of boundary condition. The microscopic models are then driven by applying boundary conditions which are consistent with macroscopic variables. Usually the values and gradients of the U are calculated from finite differences with $U(x_i)$, and then the evolution of macroscopic variables still consists of lifting, microscale simulation and restriction steps as:

$$\begin{aligned}&(1)\ u(\xi_i,t), d(x_i \pm h/2,t) \leftarrow \mathcal{R}[U(x_i \pm h/2,t), \partial U(x_i \pm h/2,t), \ldots]\\&(2)\ u(\xi_i, t+\delta t) = u(\xi_i,t) + \delta t f[u(\xi_i,t), d(x_i \pm h/2,t)]\\&(3)\ U(x_i, t+\delta t) \leftarrow \mathcal{C}[u(\xi_i, t+\delta t)]\end{aligned} \tag{42}$$

Here ξ_i represents the spatial coordinate inside the ith microscale computational cell, and the compression operator $\mathcal{C}$ can be a spatial average inside the control volume. The nature of the problem should be considered when determining the boundary conditions. For example, the mass gradients should be included for the diffusion problems.

Finally, the patch dynamics, which is the combination of coarse projective integration (41) and gap-tooth scheme (42), is proposed to extend the microscopic simulations in small spatial and temporal steps into the macroscopic large spatial and temporal steps.

The coarse time stepper, coarse projective integration and gap-tooth scheme actually extend the spatial and temporal scales of microscopic simulations. The EFM has been employed in a large variety of research fields, and some applications in the field of heat transfer and fluid flow are as follows.

The coarse time stepper and coarse projective integration can be used to accelerate the microscopic simulations by extending the simulations in small intervals to large time periods. For example, the coarse time stepper was used to generate evolution principles of the state vectors based on the LBM simulations. It was applied in the bifurcation analyses of bubble flow [224], reaction-diffusion system [225] and droplet wetting processes [226]. The coarse projective integration can be used to accelerate the LBM simulations. The reconstruction operators as described in Section 4.4.1 were used to generate the distribution functions for LBM based on the macroscopic density and velocity. Then the LBM evolved for a short time step δt. The macroscopic variables are then obtained and extrapolated to a larger time step Δt. This procedure has been adopted in the LBM simulations of reaction-diffusions [227] and multiphase problems [228].

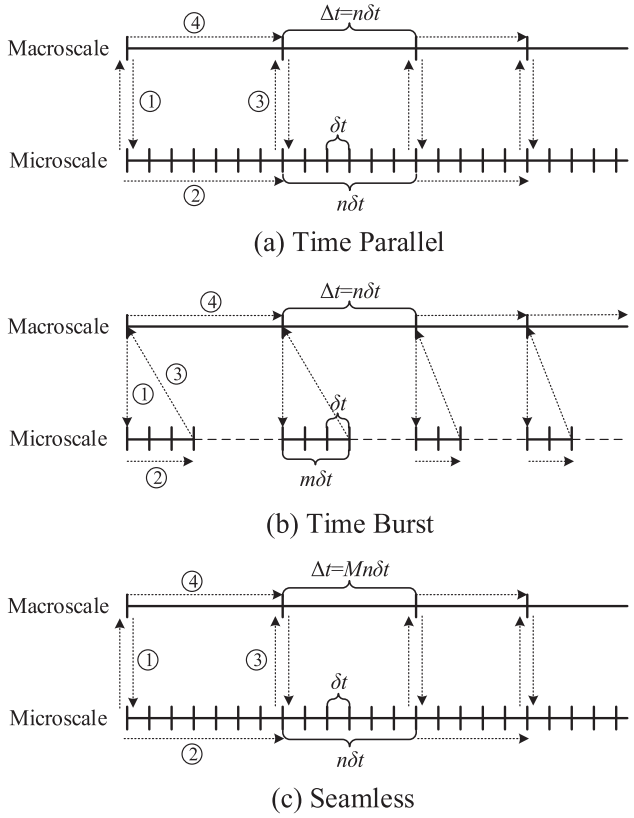

Fig. 7. Sketch of the time scale coupling schemes (① Reconstruction, ② Microscopic simulation, ③ Compression, ④ Macroscopic simulation).

The coarse projective integration can be also used to accelerate the direct numerical simulations (DNS) of the Navier–Stokes equations with the assistance of proper orthogonal decomposition (POD) [229]. The POD represents the flow fields into the following expression:

$$\mathbf{u}(\mathbf{x},t) = \sum_k a_k(t)\phi_k(\mathbf{x}) \tag{43}$$

in which $a_k(t)$ are the coefficients and $\phi_k(\mathbf{x})$ are the basis functions. Then the DNS of N–S equations is reduced into a low order model:

$$\frac{d\mathbf{a}(t)}{dt} = \mathbf{g}(t;\mathbf{a}(t)) \tag{44}$$

In the work of Sirisup et al. [229], the DNS was regarded as "microscopic" model and the evolution equation (44) of coefficients $a_k(t)$ was regarded as "macroscopic". The lifting and restriction operators are therefore given by Eq. (43). The initial velocity field was firstly generated by Eq. (43) from known $a_k(t)$. Then the DNS was adopted in small time step δt to get the new velocity field and the $a_k(t+\delta t)$. The $\mathbf{g}$ was estimated by finite difference and the $a_k(t)$ can therefore evolve for longer time steps. The same procedure was also used by Esfahanian and Ashrafi [230] to accelerate the simulations of the shallow water equations.

The coarse projective integration is also used in the simulation of the demixing in dense gas-fluidized beds [231]. The particle-based simulations are time-consuming and the EFM can be used to accelerate the simulations. In the work of Moon et al. [231], the particle-based computation was considered as "microscopic" model, and the "macroscopic" state variable was the inverse cumulative distribution function (ICDF), which is a function of volume fraction. The restriction operator was to calculate the ICDF from particle simulations. The lifting process was to generate an initial particle distribution based on the given ICDF (volume fraction), which was done by switching particle indices between different components based on the particle locations from previous step. Therefore, the particle-based simulations were conducted in small time steps. The changing rate of ICDF was obtained and the ICDF was projected to a future time with larger time steps.

The above survey of EFM demonstrates that the main feature of EFM can be regarded as an efficient method to accelerate the "microscopic" simulations. The microscopic results are restricted to several macroscopic state variables, so that the number of degree of freedom was reduced. The initial conditions of microscopic simulations are firstly generated by lifting operators under the constraints of state variables. The microscopic models evolve in small time intervals and the corresponding state variables are calculated by the restriction operators. Then the changing rates of the state variables are obtained, and the state variables are projected into future with larger time steps to accelerate the simulation.

6. Time scale coupling schemes

In the above two sections the domain decomposition multiscale methods and hierarchical multiscale methods are reviewed separately. However, the discussion is mainly on the information

transfer between methods with different length scales, and the coupling for different time scales is not specially considered. In this section, the coupling schemes for time scales are introduced and briefly discussed.

A general classifications of time scale coupling schemes can be found in the work of Lockerby et al. [93] and Scheibe et al. [79]. Based on the survey of existing multiscale methods in this work we further divide the time coupling schemes into three categories: time parallel scheme, time burst scheme and seamless scheme, and their sketches are shown in Fig. 7. The computational procedures are also numbered in Fig. 7. It can be seen that all the schemes contain four steps: reconstruction, microscopic simulation, compression and macroscopic simulation. The procedures have been described at the end of Section 3.

The time parallel scheme is applied to the problems when there is no significant temporal scale separation. Both the macroscopic and microscopic simulations span the whole time line. The microscopic time step is δt and the macroscopic time step is $\Delta t = n\delta t$. The n is the ratio between two time steps and it can be variable during the simulation. The information exchange between the two methods occurs at specific time steps. Since the microscopic simulation span the whole simulation time, the computational cost of the microscopic model should be acceptable. Therefore, the overall time-span of the simulation is limited by the microscopic method. If the microscale is atomistic MD simulation, the time of the problem should be also in atomistic scale such as nanoseconds. For example, the time parallel scheme is used in the coupling simulations of nanoscale unsteady Couette flows [114]. If the microscale is mesoscopic LBM simulation, whose time steps are suitable for the large-scaled thermo-fluid simulations, the coupling simulation can be also employed for large time scale. For example, Tong et al. [173] extended the coupled FVM-LBM methods to unsteady simulations by a time parallel scheme. Another issue about the time parallel scheme is that in the numerical methods like MD, DSMC and LGA, the temporal average is needed to obtain the macroscopic variables, so the time point of the variables is the middle time of the sampling period, which is different from the time of the system. Therefore, the special treatments of the sampling and average processes are needed. For example, Delgado-Buscalioni and Coveney discussed the differences between synchronized and sequential time coupling for atomistic-continuum coupling [114]. In synchronized coupling both the MD and continuum are advanced synchronously, so the macroscopic variables of MD has a delay of Δt. In sequential coupling the MD is advanced one more Δt time step, so the macroscopic variables are synchronized. They argued that the sequential coupling is more suitable for serial simulation and the synchronized coupling is more suitable for parallel simulation.

If there is a separation of time scale between processes in different scales and the relaxation time τ_ε is much smaller than Δt, the time burst coupling scheme can be used. In this scheme, the microscopic model evolves for $m\delta t$ corresponding to every macroscopic time step. The period $m\delta t$ should be larger than τ_ε so that the initial artificial effects of the microscopic model can be relaxed and the model reaches a quasi-equilibrium state. The $m\delta t$ should also be smaller than the Δt. The above reviews of the HMM and EFM show that the time scale separation and time burst method are the major components of the methods. In HMM the microscopic model evolves to a quasi-equilibrium state under the constraint of the macroscopic variables and then provides the missing parameters and variables to the macroscopic simulation for next Δt step. In the EFM it is assumed that when $m\delta t$ is larger than τ_ε the higher moments that are incorrectly initialized are healed. Then the coarse projective integration is used to extrapolate the short time step to longer time step Δt. The time burst scheme is also adopted in the domain decomposition methods for unsteady simulations. For example, Liu et al. [232] used the time burst scheme to propose a multi-timescale algorithm for the atomistic-continuum coupling. The MD is simulated in two shorter time intervals and the changing rates of macroscopic values can be determined. Then the values for next macroscopic step are extrapolated. It should be mentioned that the time burst scheme is also valid for the coupling simulations for steady state problems. The simulation time of macroscopic and microscopic methods can be different and both the methods can reach quasi-equilibrium states before the information is exchanged.

E et al. [90–92] argued that in the time burst scheme the microscopic models need to be reinitialized before every burst of microscopic calculation. The reinitialization procedures cost many computational resources. Therefore they proposed the seamless method in which the microscopic model evolves continuously and the reinitialization is prevented. The basic ideal is to use different time scales. Similar to the time burst scheme, the microscopic model still needs to evolve for $n\delta t$ to achieve the requirement of relaxation $n\delta t > \tau_\varepsilon$. The difference is that the macroscopic time step Δt needs not to be consistent with $n\delta t$, and it can be a much larger time step $\Delta t = Mn\delta t$. Also similarly to time parallel scheme, the two methods exchange information at specific time steps and the microscopic model evolves continuously. Therefore, the scheme can be regarded as that the macroscopic model drives the microscopic model.

In the original works of E et al. [90–92], if the microscopic $N\delta t$ is equal to the macroscopic Δt, the macroscopic time step is set to $\Delta t/N$ so that the two methods exchange information every microscopic time step. Lockerby et al. [93] generalized the model by allowing each macroscopic time step correspond to several microscopic time step $n\delta t$. In Fig. 7(c) this general scheme is used and we still call it seamless method.

Mathematically, if the evolution equations are described by Eqs. (20) and (21), the seamless method follows the following procedures:

$$\begin{aligned}
&(1)\ k = 1 \ \sim\ n : d^{(i,k)} \leftarrow U^{(i)}, u^{(i,k)} = u^{(i,k-1)} + \delta t f\left(u^{(i,k-1)}; d^{(i,k)}\right)\\
&(2)\ u^{(i+1,0)} \leftarrow u^{(i,n)}\\
&(3)\ D^{(i+1)} \leftarrow u^{(i+1,0)}\\
&(4)\ U^{(i+1)} = U^{(i)} + \Delta t F\left(U^{(i)}; D^{(i+1)}\right)
\end{aligned} \tag{45}$$

The first two steps represent the reconstruction and microscopic evolution, the third and forth steps are compression and macroscopic evolution. The Δt equals $Mn\delta t$ with $M \gg 1$.

From the other point of view, the seamless method has the same feature as the "amplification" technique which was described by Chopard et al. [81], in which the evolution rate of the macroscopic slow process is accelerated to avoid a great number of the calculation of the microscopic fast processes. Here the macroscopic evolution equation is changed to:

$$\partial_t U = MF(U; D) \tag{46}$$

Then the step 4 of procedure changes into

$$(4)\ U^{(i+1)} = U^{(i)} + n\delta t \cdot MF\left(U^{(i)}; D^{(i+1)}\right) \tag{47}$$

Under this condition both the macroscopic and microscopic methods have the same time step. It is easy to see that Eq.(47) is equivalent to the step 4 of procedure (45). After the simulation, the time of macroscopic models should be rescaled by multiplying the ratio M. This point of view also demonstrates that the time scale separation is critical for the seamless scheme, since it is assumed that the macroscale evolution with either the original

rate or the amplified rate has few influence on the microscopic process. This means that the microscopic process relaxes quickly in $n\delta t$ steps.

Finally, in order to further demonstrate the differences among these schemes, the numerical simulation of fouling processes on the tubes of heat exchangers are used as an example [179,233]. In the problem the ash particles are carried by the air flow to the surface of the tubes. Then the particles collide with the surface and the reflection, deposition and removal may occur based on the impacting velocity and material properties. With the deposition of particles, the fouling layer grows and changes the boundary of flow. If the particle-surface collision process is assumed to be instantaneous, there are major two time scales for the process. One is the air flow and particle motion. The time scale is compatible with the period of vortex shedding behind the tubes, which is tens of microseconds [233]. The other is the growth of fouling layer, which can be minutes, hours and even days. The two time scales differ by several orders of magnitudes. A straightforward idea is to simulate the fouling process with the time step of the flow field simulation. This can be regarded as the time parallel scheme. However, since the unsteady flow simulation with high Reynolds number needs a lot of computation, the time parallel scheme is not suitable for this problem.

Pérez et al. [233] used the time burst scheme to attack the problem. They simulated the air flow, particle motion and deposition process for a period of $10{\cdot}T$. Here T refers to the period of vortex shedding. The mass of deposited particles in this period is counted and the deposition rate is obtained. This rate is further use to get the mass of deposition in longer time step $\Delta t \gg 10{\cdot}T$. Then the shape of the fouling layer is evolved for Δt time step as the new boundary for the flow simulation.

On the other hand, the method proposed by Tong et al. [179] can be regarded as a seamless scheme. They accelerated the fouling process by a time ratio t_r, which is related to the parameters used in the simulation. They also proved that when the t_r is small enough (still much larger than 1), the tuning of t_r has few effects on the fouling process. Therefore, the fouling process can be simulated within an affordable period of flow simulation. After the simulation, the simulated time is rescaled by t_r to get the real time period.

7. Discussions and further developments

In the above sections, the numerical methods in macroscale, mesoscale and microscale are reviewed and a framework for multiscale simulation is proposed. Based on this framework, the current researches on the two categories of multiscale methods, domain decomposition and hierarchical method, are reviewed. Finally the time coupling scheme is reviewed. Based on the above survey of multiscale numerical methods, some discussions about the current state of multiscale simulations and the future developments are presented in this section.

(1) The terminology of multiscale simulations

The first issue about the multiscale numerical methods is its current diversity of terminology. For example, the information exchange procedures between numerical methods in different scales are called reconstruction-compression [73], lifting-restriction [77] or aggregation-disaggregation [85]. The coupled or hybrid method often refers to domain decomposition method in the studies such as the multiscale atomistic-continuum methods [97]. The embedded scheme has the same characteristics as the HMM [73] or point-wise-coupling [86]. Also, the hierarchical method, serial method or sequential method are often used for the same meaning. This diversity comes from the multidisciplinary feature of the multiscale modeling. Researches may focus on different aspects of the multiscale methods and use different terminologies. However, this diversity of terminology will not cause ambiguous in the researches and the meanings are clear according to the context. The more important issue is the characteristics of the different multiscale methods, and the criteria for the choice of methods. The Section 3 has been dedicated to these problems. We suggest the degree of the spatial and temporal separation, the coupling strength between the methods and the knowledge about macroscopic model as the main characteristics to distinguish and choose the multiscale methods.

(2) The spatial and temporal scale separation as important conditions for multiscale methods

From the framework in Section 3, it can be seen that spatial scale separation is essential for both the domain decomposition and hierarchical methods. In the domain decomposition the microscopic domain should be small so that it is suitable for microscopic methods. In the hierarchical methods the information that needed to be extracted from the microscopic simulations should be well defined in small space so that the microscopic models can be applied locally.

When the spatial scale separation is not significant, the microscopic methods should be applied in the whole computational domain. As mentioned in Section 3, the traditional multiscale methods such as multigrid method (MG) and adaptive mesh refinement (AMR) can be used. E et al. [21,75] categorized these traditional approaches and domain decomposition methods into linear scaling algorithms, in which the computational complexity scales linearly with the number of degrees of freedom for the microscopic model that is needed to resolve the problem. The hierarchical multiscale methods reviewed are categorized into sublinear scaling algorithms, in which the computational complexity scales sublinearly with the necessary number of degrees of freedom for microscale solution. According to the literature review in the previous sections, we could figure out two major differences between the multiscale methods mentioned in the present work and the traditional MG and AMR methods. The first is that the microscale region are not fully-resolved by microscopic methods as mentioned above. The second is that there are two or more levels of models that are solved respectively and coupled together by information exchange. Thus, the utilization of the spatial scale separation can be regarded as the main characteristic for the multiscale methods reviewed in the present work.

The scale separation of time is also discussed in Section 6. Similarly, the multiscale methods can take advantages of the temporal scale separation to reduce the calculation of microscopic models. When the time steps of microscopic models are suitable for the simulation of the whole process, the time parallel scheme can be used. For the steady state problems the time step of macroscale and microscale can be decoupled and both methods can evolve to quasi-equilibrium states before information exchange.

(3) The role of mesoscopic methods in multiscale methods

In Section 2.3 several particle-based mesoscopic methods are mentioned, which include DSMC, LGA/LBM and DPD/SDPD. The DSMC is different from the other methods because its evolution mechanism is developed directly from the kinetic theory. The statistical sampling of the collision is designed to simulate the collision term of Boltzmann equation. The DSMC also has a specific field of application – the rarefied gas flow. On the other hand, the LGA and DPD are firstly developed heuristically with a physicist intuition [64]. In these methods it is assumed that the hydro-

dynamics behaviors are not sensitive to the detailed microscopic mechanism, so the LGA evolves in a regular lattice with simple collision rules, and the DPD adds dissipative and random interactions to MD. These methods can be regarded as bottom-up because the macroscopic behaviors are generated from intuitive models in mesoscale. Although these heuristic developments have good physical insights, the drawbacks also exist. The LGA suffers statistical error, lack of Galilean invariance and complex collision operator. The DPD has difficulty in specifying equation of state, transfer coefficient and physical scale. In order to solve these drawbacks, these mesoscopic methods are rechecked and their relations to the macroscopic behaviors are studied. Then the LGA and DPD experience the same top-down trend of development. The SDPD is constructed directly from hydrodynamic equations. The LGA evolves into LBM and the Chapman-Enskog expansions are used to relate LBM to macroscopic governing equations. Then many lattice Boltzmann models are constructed top-down by tuning the components of the models, so that the recovered macroscopic equations are in consistent with macroscopic governing equations. Some examples are the temperature distribution functions for heat transfer and the LBM for flows in porous media [234,235].

This top-down point of view sets up rigorous theoretical backgrounds for the methods, but it also drives the mesoscopic models close to the macroscopic models. The LBM is sometimes regarded as an alternative CFD solver. Therefore, one may ask that whether the researches on the multiscale models with mesoscopic methods are still needed, especially when the coupling models between macroscopic methods and microscopic methods are widely studied. What is the advantages of using mesoscopic models, especially DPD and LBM, in multiscale models?

From the literature review in this work, especially the coupling scheme reviewed in Section 4, we can conclude that the valuable mesoscopic natures facilitate the multiscale modeling. For example, the particulate nature of DPD/SDPD makes the AdResS possible for the coupling with MD. The mesoscopic velocity distribution functions of LBM facilitate its coupling with DSMC and MD. Therefore, although the top-down point of view ensure the rigor of the mesoscopic methods, the bottom-up point of view is more valuable for the multiscale models. More attentions can be paid to the relations between mesoscopic methods and the microscopic or mesoscopic theories. For example, the extension of LBM to strong non-equilibrium flow regions based on kinetic theory has the potential for future down-coupling with "true" Boltzmann equation or MD [57]. The understanding of bottom-up relations between MD and DPD will also help to build the coupling between MD and DPD [64]. It is expected that the intuitive linear transition of forces in AdResS can have more theoretical background and the coupling can be extended to non-isothermal simulation.

(4) The discussions about domain decomposition scheme

In the present work a lot of efforts have been attribute to the review of the multiscale method based on the domain decomposition framework. Part of the reason for this extensive research interest is that the information exchange schemes in domain decomposition clearly exhibit the relations between numerical methods in different scales. These relations are fundamental for the further development of multiscale models. However, the domain decomposition scheme also has its drawbacks.

One of the drawbacks is already mentioned in this paper, and as Borg et al. [121] have described it: the application of domain decomposition needs a scale separation in all the dimensions. E et al. [75] also limited the domain decomposition to type A problem, in which the problem contains singularities that should be simulated from microscale. In this work, we state the condition for the utilization of domain decomposition is that the size of the microscopic region is suitable for the microscopic simulation. More clearly, since the microscopic models still consume most of the computation in the domain decomposition methods, the computational cost of the microscopic models should be acceptable. Therefore, the size of microscopic region should not be too large comparing with the spatial step of the microscopic method. Similar request is also needed for temporal scale if there is no significant scale separation.

This precondition is a limitation for the domain decomposition scheme. For example, one cannot use domain decomposition for the flow in a long nano-channel because the MD cannot be applied along the whole boundary region of the channel [121]. The utilization of coupled LBM-FVM for the transport processes in fuel cells is also limited to the length scale of millimeters, because the fully resolved porous structures of the electrodes need large amount of LBM simulations [171,176]. On the other hand, the coupled DSMC-continuum methods can be used to study the rarefied gas flow around structures in meters because the DSMC itself is suitable for these problems [149,150]. Therefore, it seems that the scale of the domain decomposition scheme is dominated by the microscopic methods, and this scheme does not significantly extend the scale of microscopic simulations, but only saves the computation cost by coupling with macroscopic methods.

It should be mentioned that in the other field of researches, the domain decomposition scheme has shown its applications. It has been used to develop multiscale methods spanning from continuum to quantum mechanics for the simulation of dynamic fracture [236]. The tight-binding method is used at the crack tip, which is surrounded by a MD region, and then a FEM region for far-field. Also, the coupled quantum mechanical and molecular mechanical model has been widely used in the chemical and biophysical systems, in which the quantum mechanics is employed in the reaction region [237]. In thermo-fluid systems there are similar singularity problems such as shock waves and boundaries, but usually the scale separation is limited to one dimension and the complexity is generated for high dimensional simulations. Therefore, the well-defined local singularity problems such as crack tip and reaction molecules in enzyme are not common in the thermo-fluid systems. This can be one of the reasons that limits the application of domain decomposition scheme.

A promising way to extend the application of domain decomposition scheme is to combine this scheme with the other multiscale frameworks. It should be mentioned that the information transfer methods from continuum to MD for domain decomposition have already been used in the embedded simulations [74,205,207]. As a more specific example, Vu et al. [238] combined the domain decomposition scheme and the embedded scheme for the hybrid MD-continuum simulations of flows in micro-channels. In their work the MD was used in the boundary region of channel, and coupled with continuum method for the simulation of inner area. However, instead of applying MD along the whole channel boundary, the domain decomposition coupling simulation was adopted in several blocks along the boundary, and the macroscopic values between the blocks were interpolated. Still, the Couette flow and heat conduction between two plates were used to validate the model. This combined method uses domain decomposition scheme to couple numerical methods in different scales, and uses the embedded scheme to extend the length scale of the computation. The extensions of this combination to more complex geometries and applications are still needed.

Also, the domain decomposition can be combined with the adaptive mesh scheme to reduce the utilization of microscopic models, such as in the coupling between DSMC and continuum methods. The regions described by microscopic models are changed and optimized during the simulation. In order to effectively employ the adaptive mesh, the criteria for the determination of

the breakdown of macroscopic methods are needed. However, in the present researches only the coupling between DSMC and continuum has clear breakdown parameters based on the *Kn* number. In other coupling simulations the position of the interface are seldom systematically studied. Therefore, the improvement of the domain decomposition scheme is based on the deeper understandings of the numerical methods in different scales. The clarifications of the breakdown conditions of different models are needed.

(5) Reducing the microscopic computations

Although the multiscale frameworks can reduce the computation of microscopic methods, the microscopic calculations still consumes large amount of the computation. Therefore, to reduce the microscopic calculations can greatly increase the efficiency of multiscale numerical methods. As mentioned in Section 3, the difference between the serial scheme and the embedded scheme is the knowledge about the macroscopic models. When the macroscopic models become more complex, there are less knowledge about the models, and the microscopic computations change from separate pre-calculations to the "on-the-fly" concurrent simulations. The degree of freedom of the model increases and thus the amount of microscopic computations increases correspondently.

For the serial multiscale methods, when the closure forms of macroscopic relations are obtained, the microscopic pre-calculations should be well designed to obtain the parameters of the macroscopic relations efficiently. More complex condition is the embedded multiscale methods. The traditional idea here is to firstly reduce the number of positions that the microscopic simulations are needed, and secondly reduce the number of microscopic simulations in each position. The first can be solved by using adaptive mesh or adaptive sampling techniques [239]. The second problem relays on the reduced-order models for microscopic simulations [202]. For example, the aforementioned POD can be used to generate reduced-order models of for the multiscale simulations of the cooling of data center [240–242]. The POD decomposes the temperature or velocity fields in the domain into a linear combination of optimal modes, then the calculation of new fields can be simplified into the calculation of the POD coefficients for each modes. Therefore, the number of degrees of freedom is reduced. Nie and Joshi [240] developed the POD model for a single server enclosure, and then combined the enclosure models to simulate the heat transfer and flow in the entire cabinet. The applications of EFM as described in Section 5.3 are also good examples for the reduced-order simulations.

Recently, the rapid developing artificial intelligence and machine learning techniques also shed light on the model reduction in multiscale simulations. It has been mentioned that one of the complexities of the embedded scheme comparing with the serial scheme is the unknown complex constitutive laws. From this point of view, the neutral network (NN) has been trained to generate these complex and nonlinear relations based on pre-calculations. For example, the NN was used to relate the turbulent viscosity coefficient in the large eddy simulation to the velocity derivatives and fluctuations [243]. The NN was also used to derive closure forms of gas flux and streaming stresses for the one-dimensional bubble flow. The void fraction, the gradients of the void fraction and velocity were chosen as arguments of the relations [244]. In a more complex condition when the wall effects were considered, the relation for average surface tension was also trained and the distance to the wall was added to the arguments [245].

Another complexity of the embedded scheme comparing with the serial scheme is that the microscopic computations are repeated during the simulation, although most of the calculations are under similar conditions. From this point of view, the machine learning can also help to avoid the repetition of microscopic computations for the on-the-fly coupling. For example, Asproulis and Drikakis [246] combined the NN model with the embedded scheme for the coupling between MD and continuum model. Instead of applying MD calculations for every set of macroscopic variables, the MD results were saved in a library and the artificial neural networks were trained based on the library. In their simulations of heat transfer in Couette flow, the inputs of the NN were the continuum velocity and temperature, and the outputs were the slip velocity and the temperature jump on the boundary. The confidence interval was given before the simulation. Every time the MD calculation was needed, the corresponding macroscopic variable inputs were compared with the library. If the inputs were inside the confidence interval of a set of data in the library, the NN was adopted. Otherwise, the exact MD simulation was executed, the results were stored in the library and the NN was retrained and updated. Stephenson et al. [247] improved the model by using the Gaussian process to model the MD library. The Bayesian inference was employed for the criterion for the new MD calculation, and the ad hoc fixed confidence interval was prevented. Roehm et al. [248] also used the cloud database to store the MD results and applied the kriging to estimate the unknown values for the HMM simulations. Finally, it should be mentioned that the physical considerations such as symmetry and Galilean invariance can still be used to find the inputs of the NN.

Therefore, the machine learning shortens the distance between embedded scheme and the serial scheme by either constructing complex non-linear closure relations before simulation or updating the relations on-the-fly. The combination with machine learning techniques is a promising method to reduce the microscopic calculations and improve the efficiency of multiscale simulations. However, the combination should also be carefully used because the physics inside the microscopic models are lost in the machine learning processes.

(6) Extending the applications of multiscale methods

Based on the review of the current state of the multiscale simulation, it can be seen that although the serial scheme has been used in the practical engineering problems, the applications of the other schemes are still limited. For the domain decomposition scheme, embedded scheme and the equation-free scheme, majority of the researches still focus on the coupling schemes for information exchanges, and the proposed schemes are validated by simple examples which include the steady and unsteady 1D shear flows and heat conductions, 2D benchmarks such as the lid-driven flows.

The simplicity of the serial scheme bases on two aspects. Firstly, it is a direct combination of the mature numerical methods in different scales. The microscopic simulations are used to substitute the experiments to determine the parameters for the macroscopic models. Therefore, the information transfer is parameterized and the numerical methods can be regarded as decoupled. The complexity of the state and flux exchange between different numerical methods are prevented. Secondly, the microscopic pre-calculations can be employed separately, so the demand of microscopic calculations is largely reduced.

On the other hand, the other schemes are not simple combinations of the existing numerical methods. As extensively reviewed in Section 4, the two-way information exchange between different numerical methods need special considerations based on the characteristics of the methods. Also, the concurrent coupling requires the microscopic simulations to be calculated on-the-fly, so the amount of microscopic calculations is large. However, these schemes actually couple the numerical methods in different scales and the exhibit the spirit of the multiscale simulations. These "coupling simulations" are the future of multiscale simulations.

Fortunately, based on the extensive researches on the coupling schemes between different methods, the information exchange techniques have been established for many numerical methods in different scales. Plenty of weapons have been made to attack the multiscale problems and our arsenal is still expanding. As for the computational costs of microscopic methods, we believe that with the increasing understanding of the spatial and temporal coupling schemes, the rapid developments of high performance parallel computation of microscopic methods, and the combination of adaptive mesh techniques and reduced-order models such as machine learning, the limitations of microscopic methods on the multiscale simulations can be reduced in the future.

Finally, as Fish has stated [202], "most new technologies began with a native euphoria" when the inventions were overpromised. The rapid development led to a "peak of hype" and followed by a period of crash when the immaturity of the ideas was overreacted. Then, only the technologies that were found to have a "good use" survived. We believe that along with the extensive fundamental researches on the numerical methods, it is the time to introduce the multiscale methods, especially the "coupling methods", to the applications on more practical multiscale heat transfer and fluid flow problems. Both the fundamental and practical researches will benefit from this applications, and the multiscale simulations will have a promising future.

Conflict of interest

The authors declared that there is no conflict of interest.

Acknowledgements

This work is supported by the National Key R&D Program of China (2018YFB0605901) and the Key Project of National Natural Science Foundation of China (No. 51436007).

The authors would also like to thank the Foundation for Innovative Research Groups of the National Natural Science Foundation of China (No. 51721004).

References

[1] S. Alkharabsheh, J. Fernandes, B. Gebrehiwot, D. Agonafer, K. Ghose, A. Ortega, Y. Joshi, B. Sammakia, A brief overview of recent developments in thermal management in data centers, J. Electron. Packag. 137 (4) (2015) 040801.
[2] X.R. Wei, G.X. Wang, P. Massarotto, S.D. Golding, V. Rudolph, Numerical simulation of multicomponent gas diffusion and flow in coals for CO_2 enhanced coalbed methane recovery, Chem. Eng. Sci. 62 (16) (2007) 4193–4203.
[3] F. Javadpour, D. Fisher, M. Unsworth, Nanoscale gas flow in shale gas sediments, J. Can. Pet. Technol. 46 (10) (2007) 55–61.
[4] R.S. Middleton, G.N. Keating, P.H. Stauffer, A.B. Jordan, H.S. Viswanathan, Q.J. Kang, J.W. Carey, M.L. Mulkey, E.J. Sullivan, S.P. Chu, R. Esposito, T.A. Meckele, The cross-scale science of CO_2 capture and storage: from pore scale to regional scale, Energy Environ. Sci. 5 (6) (2012) 7328–7345.
[5] H. Yoon, Q. Kang, A. Valocchi, Lattice Boltzmann-based approaches for pore-scale reactive transport, Rev. Mineral. Geochem. 80 (1) (2015) 393–431.
[6] M. Andersson, J. Yuan, B. Sundén, Review on modeling development for multiscale chemical reactions coupled transport phenomena in solid oxide fuel cells, Appl. Energy 87 (5) (2010) 1461–1476.
[7] K.N. Grew, W.K.S. Chiu, A review of modeling and simulation techniques across the length scales for the solid oxide fuel cell, J. Power Sources 199 (2012) 1–13.
[8] Y.L. He, T. Xie, Advances of thermal conductivity models of nanoscale silica aerogel insulation material, Appl. Therm. Eng. 81 (2015) 28–50.
[9] P.W. Anderson, More is different, Science 177 (4047) (1972) 393–396.
[10] G.K. Batchelor, An Introduction to Fluid Dynamics, Cambridge University Press, Cambridge, 2000.
[11] J.C. Slattery, Momentum, Energy, and Mass Transfer in Continua, second ed., Krieger Publishing Company, NewYork, 1981.
[12] S. Paolucci, Continuum Mechanics and Thermodynamics of Matter, Cambridge University Press, Cambridge, 2016.
[13] S. Chapman, T.G. Cowling, The Mathematical Theory Of Non-Uniform Gases, third ed., Cambridge University Press, Cambridge, 1970.
[14] J.H. Ferziger, M. Peric, Computational Methods for Fluid Dynamics, third ed., Springer, Heidelberg, 2002.
[15] J. Fish, T. Belytschko, A First Course in Finite Elements, John Wiley & Sons, 2007.
[16] S.V. Patankar, Numerical Heat Transfer and Fluid Flow, McGraw-Hill, New York, 1980.
[17] R.A. Gingold, J.J. Monaghan, Smoothed particle hydrodynamics: theory and application to non-spherical stars, MNRAS 181 (3) (1977) 375–389.
[18] L.B. Lucy, A numerical approach to the testing of the fission hypothesis, Astronom. J. 82 (1977) 1013–1024.
[19] G.R. Liu, M.B. Liu, Smoothed Particle Hydrodynamics: A Meshfree Particle Method, World Scientific, New Jersey, 2003.
[20] M. Gad-el-Hak, The fluid mechanics of microdevices—the Freeman scholar lecture, J. Fluids Eng. 121 (1) (1999) 5–33.
[21] E W. Principles of multiscale modeling, Cambridge University Press, Cambridge, 2011.
[22] D.C. Rapaport, The Art of Molecular Dynamics Simulation, second ed., Cambridge University Press, Cambridge, 2004.
[23] S.D. Stoddard, J. Ford, Numerical experiments on the stochastic behavior of a Lennard-Jones gas system, Phys. Rev. A 8 (3) (1973) 1504–1512.
[24] M.P. Allen, D.J. Tildesley, Computer Simulation of Liquids, Oxford University Press, 1987.
[25] T.R. Teschner, L. Könözsy, K.W. Jenkins, Progress in particle-based multiscale and hybrid methods for flow applications, Microfluid. Nanofluid. 20 (4) (2016) 68.
[26] G.M. Kremer, An Introduction to the Boltzmann Equation and Transport Processes in Gases, Springer, Heidelberg, 2010.
[27] G.A. Bird, Molecular Gas Dynamics and the Direct Simulation of Gas Flow, Clarendon Press, Oxford, 1994.
[28] H. Grad, On the kinetic theory of rarefied gases, Commun. Pure Appl. Math. 2 (4) (1949) 331–407.
[29] H. Grad, Note on N-dimensional Hermite polynomials, Commun. Pure Appl. Math. 2 (4) (1949) 325–330.
[30] P.L. Bhatnagar, E.P. Gross, M. Krook, A model for collision processes in gases. I. Small amplitude processes in charged and neutral one-component systems, Phys. Rev. 94 (3) (1954) 511–525.
[31] C. Shen, Rarefied Gas Dynamics: Fundamentals, Simulations and Micro Flows, Springer, Heidelberg, 2006.
[32] G.A. Bird, Molecular Gas Dynamics, Clarendon Press, Oxford, 1976.
[33] J. Hardy, Y. Pomeau, O. De Pazzis, Time evolution of a two-dimensional model system. I. Invariant states and time correlation functions, J. Mathem. Phys. 14 (12) (1973) 1746–1759.
[34] J. Hardy, O. De Pazzis, Y. Pomeau, Molecular dynamics of a classical lattice gas: transport properties and time correlation functions, Phys. Rev. A 13 (5) (1976) 1949.
[35] U. Frisch, B. Hasslacher, Y. Pomeau, Lattice-gas automata for the Navier-Stokes equation, Phys. Rev. Lett. 56 (14) (1986) 1505.
[36] D.A. Wolf-Gladrow, Lattice-gas Cellular Automata and Lattice Boltzmann Models: An Introduction, Springer, Heidelberg, 2000.
[37] S. Succi, The Lattice Boltzmann Equation for Fluid Dynamics and Beyond, Clarendon Press, Oxford, 2001.
[38] S. Chen, G.D. Doolen, Lattice Boltzmann method for fluid flows, Annu. Rev. Fluid Mech. 30 (1) (1998) 329–364.
[39] G.R. McNamara, G. Zanetti, Use of the Boltzmann-equation to simulate lattice-gas automata, Phys. Rev. Lett. 61 (20) (1988) 2332–2335.
[40] F.J. Higuera, J. Jimenez, Boltzmann approach to lattice gas simulations, Europhys. Lett. 9 (7) (1989) 663.
[41] F.J. Higuera, S. Succi, R. Benzi, Lattice gas dynamics with enhanced collisions, Europhys. Lett. 9 (4) (1989) 345.
[42] Y.H. Qian, Lattice Gas and Lattice Kinetic Theory Applied to the Navier-Stokes Equations PhD thesis, Université Pierre et Marie Curie, Paris, 1990.
[43] Y.H. Qian, D. d'Humières, P. Lallemand, Lattice BGK models for Navier-Stokes equation, Europhys. Lett. 17 (6) (1992) 479.
[44] J. Koelman, A simple lattice Boltzmann scheme for Navier-Stokes fluid flow, Europhys. Lett. 15 (6) (1991) 603–607.
[45] S. Chen, H. Chen, D. Martnez, W. Matthaeus, Lattice Boltzmann model for simulation of magnetohydrodynamics, Phys. Rev. Lett. 67 (27) (1991) 3776.
[46] Y.L. He, Y. Wang, Q. Li, Lattice Boltzmann Method: Theory and Application, Science Press, Beijing, 2009 (In Chinese).
[47] X. He, L.S. Luo, A priori derivation of the lattice Boltzmann equation, Phys. Rev. E 55 (6) (1997) R6333.
[48] X. He, L.S. Luo, Theory of the lattice Boltzmann method: from the Boltzmann equation to the lattice Boltzmann equation, Phys. Rev. E 56 (6) (1997) 6811–6817.
[49] T. Abe, Derivation of the lattice Boltzmann method by means of the discrete ordinate method for the Boltzmann equation, J. Comput. Phys. 131 (1) (1997) 241–246.
[50] X. Shan, X. He, Discretization of the velocity space in the solution of the Boltzmann equation, Phys. Rev. Lett. 80 (1) (1998) 65–68.
[51] X. Shan, X.F. Yuan, H. Chen, Kinetic theory representation of hydrodynamics: a way beyond the Navier-Stokes equation, J. Fluid Mech. 550 (2006) 413–441.
[52] P.C. Philippi, L.A. Hegele Jr, L.O.E. Dos Santos, R. Surmas, From the continuous to the lattice Boltzmann equation: the discretization problem and thermal models, Phys. Rev. E 73 (5) (2006) 056702.

[53] Q. Li, K.H. Luo, Q.J. Kang, Y.L. He, Q. Chen, Q. Liu, Lattice Boltzmann methods for multiphase flow and phase-change heat transfer, Prog. Energy Combust. Sci. 52 (2016) 62–105.
[54] A.J.C. Ladd, R. Verberg, Lattice-Boltzmann simulations of particle-fluid suspensions, J. Stat. Phys. 104 (5–6) (2001) 1191–1251.
[55] C.K. Aidun, J.R. Clausen, Lattice-Boltzmann method for complex flows, Annu. Rev. Fluid Mech. 42 (2010) 439–472.
[56] J. Zhang, Lattice Boltzmann method for microfluidics: models and applications, Microfluid. Nanofluid. 10 (1) (2011) 1–28.
[57] S. Succi, Lattice Boltzmann 2038, Europhys. Lett. 109 (5) (2015) 50001.
[58] A.C. Velivelli, K.M. Bryden, Domain decomposition based coupling between the lattice Boltzmann method and traditional CFD methods—part I: formulation and application to the 2-D Burgers' equation, Adv. Eng. Softw. 70 (2014) 104–112.
[59] A.C. Velivelli, K.M. Bryden, Domain decomposition based coupling between the lattice Boltzmann method and traditional CFD methods–Part II: numerical solution to the backward facing step flow, Adv. Eng. Softw. 82 (2015) 65–74.
[60] R.R. Nourgaliev, T.N. Dinh, T.G. Theofanous, D. Josephet, The lattice Boltzmann equation method: theoretical interpretation, numerics and implications, Int. J. Multiph. Flow 29 (1) (2003) 117–169.
[61] P.J. Hoogerbrugge, J. Koelman, Simulating microscopic hydrodynamic phenomena with dissipative particle dynamics, Europhys. Lett. 19 (3) (1992) 155–160.
[62] P. Español, P. Warren, Statistical mechanics of dissipative particle dynamics, Europhys. Lett. 30 (4) (1995) 191–196.
[63] R.D. Groot, P.B. Warren, Dissipative particle dynamics: Bridging the gap between atomistic and mesoscopic simulation, J. Chem. Phys. 107 (11) (1997) 4423–4435.
[64] P. Español, P.B. Warren, Perspective: dissipative particle dynamics, J. Chem. Phys. 146 (15) (2017) 150901.
[65] M.B. Liu, G.R. Liu, L.W. Zhou, J.Z. Chang, Dissipative particle dynamics (DPD): an overview and recent developments, Arch. Comput. Methods Eng. 22 (4) (2015) 529–556.
[66] E. Moeendarbary, T.Y. Ng, M. Zangeneh, Dissipative particle dynamics: introduction, methodology and complex fluid applications—a review, Int. J. Appl. Mech. 1 (4) (2009) 737–763.
[67] P. Español, M. Revenga, Smoothed dissipative particle dynamics, Phys. Rev. E 67 (2) (2003) 026705.
[68] N.D. Petsev, L.G. Leal, M.S. Shell, Multiscale simulation of ideal mixtures using smoothed dissipative particle dynamics, J. Chem. Phys. 144 (8) (2016) 084115.
[69] P.M. Kulkarni, C.C. Fu, M.S. Shell, L.G. Leal, Multiscale modeling with smoothed dissipative particle dynamics, J. Chem. Phys. 138 (23) (2013) 234105.
[70] A. Hoekstra, B. Chopard, P. Coveney, Multiscale modelling and simulation: a position paper, Phil. Trans. R. Soc. A 372 (2021) (2014) 20130377.
[71] G.D. Ingram, I.T. Cameron, K.M. Hangos, Classification and analysis of integrating frameworks in multiscale modelling, Chem. Eng. Sci. 59 (11) (2004) 2171–2187.
[72] E. Weinan, B. Engquist, The heterogeneous multiscale methods, Commun. Mathem. Sci. 1 (1) (2003) 87–132.
[73] E. Weinan, B. Engquist, Z. Huang, Heterogeneous multiscale method: a general methodology for multiscale modeling, Phys. Rev. B 67 (9) (2003).
[74] W. Ren, E. Weinan, Heterogeneous multiscale method for the modeling of complex fluids and micro-fluidics, J. Comput. Phys. 204 (1) (2005) 1–26.
[75] E. Weinan, B. Engquist, X. Li, W. Ren, E. Vanden-Eijnden, Heterogeneous multiscale methods: a review, Commun. Comput. Phys. 2 (3) (2007) 367–450.
[76] A. Abdulle, E. Weinan, B. Engquist, E. Vanden-Eijnden, The heterogeneous multiscale method, Acta Numer. 21 (2012) 1–87.
[77] I.G. Kevrekidis, C.W. Gear, J.M. Hyman, P.G. Kevrekidis, O. Runborg, C. Theodoropoulos, Equation-free, coarse-grained multiscale computation: enabling microscopic simulators to perform system-level analysis, Commun. Mathem. Sci. 1 (4) (2003) 715–762.
[78] I.G. Kevrekidis, G. Samaey, Equation-free multiscale computation: algorithms and applications, Annu. Rev. Phys. Chem. 60 (2009) 321–344.
[79] T.D. Scheibe, E.M. Murphy, X. Chen, A.K. Rice, K.C. Carroll, B.J. Palmer, A.M. Tartakovsky, I. Battiato, B.D. Wood, An analysis platform for multiscale hydrogeologic modeling with emphasis on hybrid multiscale methods, Groundwater 53 (1) (2015) 38–56.
[80] J. Borgdorff, J.L. Falcone, E. Lorenz, C. Bona-Casas, B. Chopard, A.G. Hoekstra, Foundations of distributed multiscale computing: formalization, specification, and analysis, J. Parallel Distrib. Comput. 73 (4) (2013) 465–483.
[81] B. Chopard, J.L. Falcone, P. Kunzli, A. Hoekstra, Multiscale modeling: recent progress and open questions, Multiscale Multidiscip. Model., Exp. Des. (2018) 1–12.
[82] B. Chopard, J. Borgdorff, A.G. Hoekstra, A framework for multi-scale modelling, Phil. Trans. R. Soc. A 372 (2021) (2014) 20130378.
[83] J. Borgdorff, M. Mamonski, B. Bosak, D. Groen, M.B. Belgacem, K. Kurowski, A. G. Hoekstra, Multiscale computing with the multiscale modeling library and runtime environment, Proc. Comput. Sci. 18 (2013) 1097–1105.
[84] J. Borgdorff, M.B. Belgacem, C. Bona-Casas, L. Fazendeiro, D. Groen, O. Hoenen, A. Mizeranschi, J.L. Suter, D. Coster, P.V. Coveney, W. Dubitzky, A.G. Hoekstra, P. Strand, Performance of distributed multiscale simulations, Phil. Trans. R. Soc. A 372 (2021) (2014) 20130407.
[85] A. Yang, W. Marquardt, An ontological conceptualization of multiscale models, Comput. Chem. Eng. 33 (4) (2009) 822–837.
[86] M. Kalweit, D. Drikakis, Multiscale simulation strategies and mesoscale modelling of gas and liquid flows, IMA J. Appl. Math. 76 (5) (2011) 661–671.
[87] D. Drikakis, M. Frank, Advances and challenges in computational research of micro-and nanoflows, Microfluid. Nanofluid. 19 (5) (2015) 1019–1033.
[88] Y.L. He, W.Q. Tao, Multiscale simulations of heat transfer and fluid flow problems, J. Heat Transf. 134 (3) (2012) 031018.
[89] Y.L. He, W.Q. Tao, Numerical solutions of nano/microphenomena coupled with macroscopic process of heat transfer and fluid flow: a brief review, J. Heat Transf. 137 (9) (2015) 090801.
[90] E. Weinan, J. Lu, Seamless multiscale modeling via dynamics on fiber bundles, Commun. Mathem. Sci. 5 (3) (2007) 649–663.
[91] W. Ren, Seamless multiscale modeling of complex fluids using fiber bundle dynamics, Commun. Mathem. Sci. 5 (4) (2007) 1027–1037.
[92] E. Weinan, W. Ren, E. Vanden-Eijnden, A general strategy for designing seamless multiscale methods, J. Comput. Phys. 228 (15) (2009) 5437–5453.
[93] D.A. Lockerby, C.A. Duque-Daza, M.K. Borg, J.M. Reese, Time-step coupling for hybrid simulations of multiscale flows, J. Comput. Phys. 237 (2013) 344–365.
[94] S. Succi, O. Filippova, G. Smith, E. Kaxiras, Applying the lattice Boltzmann equation to multiscale fluid problems, Comput. Sci. Eng. 3 (6) (2001) 26–37.
[95] P.L. Lions, On the Schwarz alternating method, in: R. Glowinski (Ed.), First International Symposium on Domain Decomposition Methods for Partial Differential Equations, SIAM, Philadelphia, USA, 1988, pp. 1–42.
[96] S.T. O'Connell, P.A. Thompson, Molecular dynamics–continuum hybrid computations: a tool for studying complex fluid flows, Phys. Rev. E 52 (6) (1995) R5792–R5795.
[97] K.M. Mohamed, A.A. Mohamad, A review of the development of hybrid atomistic–continuum methods for dense fluids, Microfluid. Nanofluid. 8 (3) (2010) 283–302.
[98] X.B. Nie, S.Y. Chen, M. Robbins, A continuum and molecular dynamics hybrid method for micro- and nano-fluid flow, J. Fluid Mech. 500 (2004) 55–64.
[99] T. Werder, J.H. Walther, P. Koumoutsakos, Hybrid atomistic–continuum method for the simulation of dense fluid flows, J. Comput. Phys. 205 (1) (2005) 373–390.
[100] R. Delgado-Buscalioni, P.V. Coveney, USHER: an algorithm for particle insertion in dense fluids, J. Chem. Phys. 119 (2) (2003) 978–987.
[101] J. Li, D.Y. Liao, S. Yip, Coupling continuum to molecular-dynamics simulation: reflecting particle method and the field estimator, Phys. Rev. E 57 (6) (1998) 7259–7267.
[102] N.G. Hadjiconstantinou, A.T. Patera, Heterogeneous atomistic-continuum representations for dense fluid systems, Int. J. Mod. Phys. C 8 (4) (1997) 967–976.
[103] J. Li, D.Y. Liao, S. Yip, Nearly exact solution for coupled continuum/MD fluid simulation, J. Comput. Aided Mater. Des. 6 (2–3) (1999) 95–102.
[104] Y.C. Wang, G.W. He, A dynamic coupling model for hybrid atomistic-continuum computations, Chem. Eng. Sci. 62 (13) (2007) 3574–3579.
[105] X.B. Nie, S.Y. Chen, M.O. Robbins, Hybrid continuum-atomistic simulation of singular corner flow, Phys. Fluids 16 (10) (2004) 3579–3591.
[106] T.H. Yen, C.Y. Soong, P.Y. Tzeng, Hybrid molecular dynamics-continuum simulation for nano/mesoscale channel flows, Microfluid. Nanofluid. 3 (2007) 665–675.
[107] J. Sun, Y.L. He, W.Q. Tao, Scale effect on flow and thermal boundaries in micro-/nano-channel flow using molecular dynamics-continuum hybrid simulation method, Int. J. Numer. Meth. Eng. 81 (2) (2010) 207–228.
[108] J. Sun, Y.L. He, W.Q. Tao, X. Yin, H.S. Wang, Roughness effect on flow and thermal boundaries in microchannel/nanochannel flow using molecular dynamics-continuum hybrid simulation, Int. J. Numer. Meth. Eng. 89 (1) (2012) 2–19.
[109] J. Liu, S.Y. Chen, X.B. Nie, M.O. Robbins, A continuum-atomistic simulation of heat transfer in micro- and nano-flows, J. Comput. Phys. 227 (2007) 279–291.
[110] J. Sun, Y.L. He, W.Q. Tao, Molecular dynamics–continuum hybrid simulation for condensation of gas flow in a microchannel, Microfluid. Nanofluid. 7 (3) (2009) 407–422.
[111] E.G. Flekkoy, G. Wagner, J. Feder, Hybrid model for combined particle and continuum dynamics, Europhys. Lett. 52 (3) (2000) 271–276.
[112] G. Wagner, E. Flekkoy, J. Feder, T. Jøssang, Coupling molecular dynamics and continuum dynamics, Comput. Phys. Commun. 147 (1–2) (2002) 670–673.
[113] R. Delgado-Buscalioni, P.V. Coveney, Continuum-particle hybrid coupling for mass, momentum, and energy transfers in unsteady fluid flow, Phys. Rev. E 67 (4) (2003) 046704.
[114] R. Delgado-Buscalioni, P.V. Coveney, Hybrid molecular-continuum fluid dynamics, Philos. Trans. Royal Soc. Lond. Series a-Mathem. Phys. Eng. Sci. 2004 (362) (1821) 1639–1654.
[115] J.P. Hansen, I.R. McDonald, Theory of Simple Liquids: with Applications to Soft Matter, fourth ed., Academic Press, 2013.
[116] W.J. Zhou, Z.Q. Yu, Z.Z. Li, Y.L. He, W.Q. Tao, Molecular dynamics–continuum hybrid simulation for the impingement of droplet on a liquid film, Numer. Heat Transf., Part A: Appl. 68 (5) (2015) 512–525.
[117] H.F. Wu, K.A. Fichthorn, A. Borhan, An atomistic–continuum hybrid scheme for numerical simulation of droplet spreading on a solid surface, Heat Mass Transf. 50 (3) (2014) 351–361.
[118] N.G. Hadjiconstantinou, Hybrid atomistic–continuum formulations and the moving contact-line problem, J. Comput. Phys. 154 (2) (1999) 245–265.

[119] N.G. Hadjiconstantinou, Combining atomistic and continuum simulations of contact-line motion, Phys. Rev. E 59 (2) (1999) 2475.
[120] L. Guo, S. Chen, M.O. Robbins, Multi-scale simulation method for electroosmotic flows, Eur. Phys. J. Special Topics 225 (8–9) (2016) 1551–1582.
[121] M.K. Borg, D.A. Lockerby, J.M. Reese, A multiscale method for micro/nano flows of high aspect ratio, J. Comput. Phys. 233 (2013) 400–413.
[122] D.A. Fedosov, G.E. Karniadakis, Triple-decker: interfacing atomistic–mesoscopic–continuum flow regimes, J. Comput. Phys. 228 (4) (2009) 1157–1171.
[123] M. Praprotnik, L. Delle Site, K. Kremer, Adaptive resolution molecular-dynamics simulation: changing the degrees of freedom on the fly, J. Chem. Phys. 123 (22) (2005) 224106.
[124] M. Praprotnik, L. Delle Site, K. Kremer, Adaptive resolution scheme for efficient hybrid atomistic-mesoscale molecular dynamics simulations of dense liquids, Phys. Rev. E 73 (6) (2006) 066701.
[125] S. Matysiak, C. Clementi, M. Praprotnik, K. Kremer, L. Delle Site, Modeling diffusive dynamics in adaptive resolution simulation of liquid water, J. Chem. Phys. 128 (2) (2008) 024503.
[126] J. Zavadlav, S.J. Marrink, M. Praprotnik, Adaptive resolution simulation of supramolecular water: the concurrent making, breaking, and remaking of water bundles, J. Chem. Theory Comput. 12 (8) (2016) 4138–4145.
[127] J. Zavadlav, S.J. Marrink, M. Praprotnik, Multiscale simulation of protein hydration using the SWINGER dynamical clustering algorithm, J. Chem. Theory Comput. 14 (2018) 1754–1761.
[128] N.D. Petsev, L.G. Leal, M.S. Shell, Hybrid molecular-continuum simulations using smoothed dissipative particle dynamics, J. Chem. Phys. 142 (4) (2015) 044101.
[129] J. Zavadlav, M. Praprotnik, Adaptive resolution simulations coupling atomistic water to dissipative particle dynamics, J. Chem. Phys. 147 (2017) 114110.
[130] N.D. Petsev, L.G. Leal, M.S. Shell, Coupling discrete and continuum concentration particle models for multiscale and hybrid molecular-continuum simulations, J. Chem. Phys. 147 (23) (2017) 234112.
[131] S. Poblete, M. Praprotnik, K. Kremer, Site L. Delle, Coupling different levels of resolution in molecular simulations, J. Chem. Phys. 132 (11) (2010) 114101.
[132] S. Fritsch, S. Poblete, C. Junghans, G. Ciccotti, L. Delle Site, K. Kremer, Adaptive resolution molecular dynamics simulation through coupling to an internal particle reservoir, Phys. Rev. Lett. 108 (17) (2012) 170602.
[133] R. Delgado-Buscalioni, K. Kremer, M. Praprotnik, Concurrent triple-scale simulation of molecular liquids, J. Chem. Phys. 128 (11) (2008) 114110.
[134] R. Delgado-Buscalioni, K. Kremer, M. Praprotnik, Coupling atomistic and continuum hydrodynamics through a mesoscopic model: application to liquid water, J. Chem. Phys. 131 (24) (2009) 244107.
[135] D.C. Wadsworth, D.A. Erwin, One-dimensional hybrid continuum/particle simulation approach for rarefied hypersonic flows. AIAA Paper 90-1690, 1990.
[136] D.C. Wadsworth, D.A. Erwin, Two-Dimensional Hybrid Continuum/Particle Approach for Rarefied Flows. AIAA Paper 92-2975, 1992.
[137] H.S. Wijesinghe, N.G. Hadjiconstantinou, Discussion of hybrid atomistic-continuum methods for multiscale hydrodynamics, Int. J. Multiscale Comput. Eng. 2 (2) (2004).
[138] T.E. Schwartzentruber, I.D. Boyd, Progress and future prospects for particle-based simulation of hypersonic flow, Prog. Aerosp. Sci. 72 (2015) 66–79.
[139] D.B. Hash, H.A. Hassan, Assessment of schemes for coupling Monte Carlo and Navier-Stokes solution methods, J. Thermophys. Heat Transfer 10 (2) (1996) 242–249.
[140] D.B. Hash, H.A. Hassan, A decoupled DSMC/Navier-Stokes analysis of a transitional flow experiment, AIAA Paper 96-0353, 1996.
[141] D. Hash, H. Hassan, Two-dimensional coupling issues of hybrid DSMC/Navier-Stokes solvers, AIAA Paper 97-2507, 1997.
[142] R. Roveda, D.B. Goldstein, P.L. Varghese, Hybrid Euler/particle approach for continuum/rarefied flows, J. Spacecraft Rockets 35 (3) (1998) 258–265.
[143] O. Aktas, N.R. Aluru, A combined continuum/DSMC technique for multiscale analysis of microfluidic filters, J. Comput. Phys. 178 (2) (2002) 342–372.
[144] J.S. Wu, Y.Y. Lian, G. Cheng, R.P. Koomullil, K.C. Tseng, Development and verification of a coupled DSMC–NS scheme using unstructured mesh, J. Comput. Phys. 219 (2) (2006) 579–607.
[145] Q. Sun, I.D. Boyd, G.V. Candler, A hybrid continuum/particle approach for modeling subsonic, rarefied gas flows, J. Comput. Phys. 194 (1) (2004) 256–277.
[146] T.E. Schwartzentruber, I.D. Boyd, A hybrid particle-continuum method applied to shock waves, J. Comput. Phys. 215 (2) (2006) 402–416.
[147] T.E. Schwartzentruber, L.C. Scalabrin, I.D. Boyd, A modular particle–continuum numerical method for hypersonic non-equilibrium gas flows, J. Comput. Phys. 225 (1) (2007) 1159–1174.
[148] G. Abbate, C.R. Kleijn, B.J. Thijsse, Hybrid continuum/molecular simulations of transient gas flows with rarefaction, AIAA J. 47 (7) (2009) 1741–1749.
[149] T.E. Schwartzentruber, L.C. Scalabrin, I.D. Boyd, Hybrid particle-continuum simulations of hypersonic flow over a hollow-cylinder-flare geometry, AIAA J. 46 (8) (2008) 2086–2095.
[150] T.E. Schwartzentruber, L.C. Scalabrin, I.D. Boyd, Hybrid particle-continuum simulations of nonequilibrium hypersonic blunt-body flowfields, J. Thermophys. Heat Transfer 22 (1) (2008) 29–37.
[151] F. La Torre, S. Kenjereš, J.L. Moerel, C.R. Kleijn, Hybrid simulations of rarefied supersonic gas flows in micro-nozzles, Comput. Fluids 49 (1) (2011) 312–322.
[152] G.A. Bird, Breakdown of translational and rotational equilibrium in gaseous expansions, AIAA J. 8 (11) (1970) 1998–2003.
[153] I.D. Boyd, G. Chen, G.V. Candler, Predicting failure of the continuum fluid equations in transitional hypersonic flows, Phys. Fluids 7 (1) (1995) 210–219.
[154] T.D. Holman, I.D. Boyd, Effects of continuum breakdown on the surface properties of a hypersonic sphere, J. Thermophys. Heat Transfer 23 (4) (2009) 660–673.
[155] A.L. Garcia, B.J. Alder, Generation of the Chapman-Enskog distribution, J. Comput. Phys. 140 (1) (1998) 66–70.
[156] A.L. Garcia, J.B. Bell, W.Y. Crutchfield, B.J. Alder, Adaptive mesh and algorithm refinement using direct simulation Monte Carlo, J. Comput. Phys. 154 (1) (1999) 134–155.
[157] H.S. Wijesinghe, R.D. Hornung, A.L. Garcia, N.G. Hadjiconstantinou, Three-dimensional hybrid continuum-atomistic simulations for multiscale hydrodynamics, J. Fluids Eng. 126 (5) (2004) 768–777.
[158] S.V. Nedea, A.J.H. Frijns, A.A. van Steenhoven, A.J. Markvoort, P.A.J. Hilbers, Hybrid method coupling molecular dynamics and Monte Carlo simulations to study the properties of gases in microchannels and nanochannels, Phys. Rev. E 72 (1) (2005) 016705.
[159] K. Gu, C.B. Watkins, J. Koplik, Atomistic hybrid DSMC/NEMD method for nonequilibrium multiscale simulations, J. Comput. Phys. 229 (5) (2010) 1381–1400.
[160] T. Liang, W. Ye, An efficient hybrid DSMC/MD algorithm for accurate modeling of micro gas flows, Comm. Comput. Phys. 15 (1) (2014) 246–264.
[161] D.S. Watvisave, B.P. Puranik, U.V. Bhandarkar, A hybrid MD-DSMC coupling method to investigate flow characteristics of micro-devices, J. Comput. Phys. 302 (2015) 603–617.
[162] Ya-Ling He, Zi-Xiang Tong, in: Yuwen Zhang, Ya-Ling He, Coupling Scheme of Lattice Boltzmann Method and Finite Volume Method for Multiscale Numerical Simulation, Multiscale Thermal Transport in Energy Systems, 2016, Chapter 4, Nova Science Publishers, Inc., ISBN: 978-1-63485-692-8.
[163] Z.X. Tong, M.J. Li, Y.L. He, W.Q. Tao, Analysis and numerical tests of lifting relations to reconstruct LBM distribution functions for coupling simulations, Int. J. Heat Mass Transf. 107 (2017) 945–955.
[164] P. Albuquerque, D. Alemani, B. Chopard, P. Leone, Coupling a lattice Boltzmann and a finite difference scheme, in: M. Bubak, G.D. van Albada, P. M.A. Sloot, J. Dongarra (Eds.), Computational Science–ICCS 2004, Springer, Berlin, 2004, pp. 540–547.
[165] P. Van Leemput, W. Vanroose, D. Roose, Numerical and analytical spatial coupling of a lattice Boltzmann model and a partial differential equation, in: A.N. Gorban, N. Kazantzis, I.G. Kevrekidis, H.C. Ottinger, C. Theodoropoulos (Eds.), Model Reduction and Coarse-Graining Approaches for Multiscale Phenomena, Springer, Berlin, 2006, pp. 423–441.
[166] P. Van Leemput, C. Vandekerckhove, W. Vanroose, D. Roose, Accuracy of hybrid lattice Boltzmann/finite difference schemes for reaction-diffusion systems, Multiscale Model. Simul. 6 (3) (2007) 838–857.
[167] H.B. Luan, H. Xu, L. Chen, D.L. Sun, W.Q. Tao, Numerical illustrations of the coupling between the lattice Boltzmann method and finite-type macro-numerical methods, Numer. Heat Transfer Part B-Fundam. 57 (2) (2010) 147–171.
[168] H.B. Luan, H. Xu, L. Chen, D.L. Sun, Y.L. He, W.Q. Tao, Evaluation of the coupling scheme of FVM and LBM for fluid flows around complex geometries, Int. J. Heat Mass Transf. 54 (9–10) (2011) 1975–1985.
[169] H. Xu, H. Luan, Y.L. He, W.Q. Tao, A lifting relation from macroscopic variables to mesoscopic variables in lattice Boltzmann method: derivation, numerical assessments and coupling computations validation, Comput. Fluids 54 (2012) 92–104.
[170] H.B. Luan, H. Xu, L. Chen, Y.L. Feng, Y.L. He, W.Q. Tao, Coupling of finite volume method and thermal lattice Boltzmann method and its application to natural convection, Int. J. Numer. Meth. Fluids 70 (2) (2012) 200–221.
[171] L. Chen, H.B. Luan, Y.L. Feng, C.X. Song, Y.L. He, W.Q. Tao, Coupling between finite volume method and lattice Boltzmann method and its application to fluid flow and mass transport in proton exchange membrane fuel cell, Int. J. Heat Mass Transf. 55 (13–14) (2012) 3834–3848.
[172] L. Chen, Y.L. He, Q. Kang, W.Q. Tao, Coupled numerical approach combining finite volume and lattice Boltzmann methods for multi-scale multi-physicochemical processes, J. Comput. Phys. 255 (2013) 83–105.
[173] Z.X. Tong, Y.L. He, A unified coupling scheme between lattice Boltzmann method and finite volume method for unsteady fluid flow and heat transfer, Int. J. Heat Mass Transf. 80 (2015) 812–824.
[174] M.R. Salimi, M. Taeibi-Rahni, New lifting relations for estimating LBM distribution functions from corresponding macroscopic quantities, based on equilibrium and non-equilibrium moments, J. Comput. Phys. 302 (2015) 155–175.
[175] P.A. Skordos, Initial and boundary conditions for the lattice Boltzmann method, Phys. Rev. E 48 (6) (1993) 4823.
[176] L. Chen, Y.L. Feng, C.X. Song, L. Chen, Y.L. He, W.Q. Tao, Multi-scale modeling of proton exchange membrane fuel cell by coupling finite volume method and lattice Boltzmann method, Int. J. Heat Mass Transf. 63 (2013) 268–283.
[177] M.R. Salimi, M. Taeibi-Rahni, F. Jam, Heat transfer analysis of a porously covered heated square cylinder, using a hybrid Navier–Stokes–lattice Boltzmann numerical method, Int. J. Therm. Sci. 91 (2015) 59–75.

[178] M.R. Salimi, M.T. Taeibi-Rahni, F. Jam, Pore-scale simulation of fluid flow passing over a porously covered square cylinder located at the middle of a channel, using a hybrid MRT–LBM–FVM approach, Theor. Comput. Fluid Dyn. 29 (3) (2015) 171–191.
[179] Z.X. Tong, M.J. Li, Y.L. He, H.Z. Tan, Simulation of real time particle deposition and removal processes on tubes by coupled numerical method, Appl. Energy 185 (2017) 2181–2193.
[180] A. Dupuis, P. Koumoutsakos, Effects of atomistic domain size on hybrid lattice Boltzmann–molecular dynamics simulations of dense fluids, Int. J. Mod. Phys. C 18 (4) (2007) 644–651.
[181] A. Dupuis, E.M. Kotsalis, P. Koumoutsakos, Coupling lattice Boltzmann and molecular dynamics models for dense fluids, Phys. Rev. E 75 (4) (2007) 046704.
[182] J.H. Walther, M. Praprotnik, E.M. Kotsalis, P. Koumoutsakos, Multiscale simulation of water flow past a C_{540} fullerene, J. Comput. Phys. 231 (7) (2012) 2677–2681.
[183] P. Neumann, W. Eckhardt, H.J. Bungartz, Hybrid molecular–continuum methods: From prototypes to coupling software, Comput. Math. Appl. 67 (2) (2014) 272–281.
[184] P. Neumann, H. Flohr, R. Arora, P. Jarmatz, N. Tchipev, H.J. Bungartz, MaMiCo: Software design for parallel molecular-continuum flow simulations, Comput. Phys. Commun. 200 (2016) 324–335.
[185] W.J. Zhou, H.B. Luan, J. Sun, Y.L. He, W.Q. Tao, A molecular dynamics and lattice Boltzmann multiscale simulation for dense fluid flows, Numer. Heat Transfer, Part B: Fundam. 61 (5) (2012) 369–386.
[186] Z.X. Tong, M.J. Li, X. Chen, Y.L. He, Direct coupling between molecular dynamics and lattice Boltzmann method based on velocity distribution functions for steady-state isothermal flow, Int. J. Heat Mass Transf. 115 (2017) 544–555.
[187] P. Yuan, L. Schaefer, Equations of state in a lattice Boltzmann model, Phys. Fluids 18 (4) (2006) 042101.
[188] N.G. Hadjiconstantinou, A.L. Garcia, M.Z. Bazant, G. He, Statistical error in particle simulations of hydrodynamic phenomena, J. Comput. Phys. 187 (1) (2003) 274–297.
[189] G. Di Staso, H.J.H. Clercx, S. Succi, F. Toschi, DSMC–LBM mapping scheme for rarefied and non-rarefied gas flows, J. Comput. Sci. 17 (2016) 357–369.
[190] G. Di Staso, H.J.H. Clercx, S. Succi, F. Toschi, Lattice Boltzmann accelerated direct simulation Monte Carlo for dilute gas flow simulations, Phil. Trans. R. Soc. A 374 (2080) (2016) 20160226.
[191] G. Di Staso, S. Srivastava, E. Arlemark, H.J.H. Clercx, F. Toschi, Hybrid lattice Boltzmann-direct simulation Monte Carlo approach for flows in three dimensional geometries, Comput. Fluids 172 (2018) 492–509.
[192] S.I. Ngo, Y.I. Lim, M.H. Hahn, J. Jung, Y.H. Bang, Multi-scale computational fluid dynamics of impregnation die for thermoplastic carbon fiber prepreg production, Comput. Chem. Eng. 103 (2017) 58–68.
[193] S.B. Choi, H.M. Yoon, J.S. Lee, Multi-scale approach for the rheological characteristics of emulsions using molecular dynamics and lattice Boltzmann method, Biomicrofluidics 8 (5) (2014) 052104.
[194] X. Liu, Y.F. Zhu, B. Gong, J.P. Yu, S.T. Cui, From molecular dynamics to lattice Boltzmann: a new approach for pore-scale modeling of multi-phase flow, Pet. Sci. 12 (2) (2015) 282–292.
[195] A.O. Pereira, L.S. Lara, C.R. Miranda, Combining molecular dynamics and lattice Boltzmann simulations: a hierarchical computational protocol for microfluidics, Microfluid. Nanofluid. 20 (2) (2016) 36.
[196] B. Mortazavi, T. Rabczuk, Multiscale modeling of heat conduction in graphene laminates, Carbon 85 (2015) 1–7.
[197] B. Mortazavi, H. Yang, F. Mohebbi, G. Cuniberti, T. Rabczuk, Graphene or h-BN paraffin composite structures for the thermal management of Li-ion batteries: a multiscale investigation, Appl. Energy 202 (2017) 323–334.
[198] D.M. Holland, D.A. Lockerby, M.K. Borg, W.D. Nicholls, J.M. Reese, Molecular dynamics pre-simulations for nanoscale computational fluid dynamics, Microfluid. Nanofluid. 18 (3) (2015) 461–474.
[199] J. Zhang, M.K. Borg, J.M. Reese, Multiscale simulation of dynamic wetting, Int. J. Heat Mass Transf. 115 (2017) 886–896.
[200] A. Bensoussan, J.L. Lions, G. Papanicolaou, Asymptotic Analysis for Periodic Structures, North-Holland Publishing Company, Amsterdam, 1978.
[201] G. Pavliotis, A. Stuart, Multiscale Methods: Averaging and Homogenization, Springer, 2008.
[202] J. Fish, Practical Multiscaling, John Wiley & Sons, 2013.
[203] A.W. Lees, S.F. Edwards, The computer study of transport processes under extreme conditions, J. Phys. C: Solid State Phys. 5 (15) (1972) 1921–1929.
[204] S. De, J. Fish, M.S. Shephard, P. Keblinski, S.K. Kumar, Multiscale modeling of polymer rheology, Phys. Rev. E 74 (3) (2006) 030801.
[205] N. Asproulis, M. Kalweit, D. Drikakis, A hybrid molecular continuum method using point wise coupling, Adv. Eng. Softw. 46 (1) (2012) 85–92.
[206] M. Parrinello, A. Rahman, Polymorphic transitions in single crystals: a new molecular dynamics method, J. Appl. Phys. 52 (12) (1981) 7182–7190.
[207] A. Alexiadis, D.A. Lockerby, M.K. Borg, J.M. Reese, A Laplacian-based algorithm for non-isothermal atomistic-continuum hybrid simulation of micro and nano-flows, Comput. Methods Appl. Mech. Eng. 264 (2013) 81–94.
[208] A. Alexiadis, D.A. Lockerby, M.K. Borg, J.M. Reese, A particle-continuum hybrid framework for transport phenomena and chemical reactions in multicomponent systems at the micro and nanoscale, J. Heat Transfer 137 (9) (2015) 091010.
[209] S. Yasuda, R. Yamamoto, Multiscale modeling and simulation for polymer melt flows between parallel plates, Phys. Rev. E 81 (3) (2010) 036308.
[210] S. Yasuda, R. Yamamoto, A model for hybrid simulations of molecular dynamics and computational fluid dynamics, Phys. Fluids 20 (11) (2008) 113101.
[211] T. Murashima, S. Yasuda, T. Taniguchi, R. Yamamoto, Multiscale modeling for polymeric flow: particle-fluid bridging scale methods, J. Phys. Soc. Jpn. 82 (1) (2012) 012001.
[212] S. Yasuda, R. Yamamoto, Synchronized molecular-dynamics simulation for the thermal lubrication of a polymeric liquid between parallel plates, Comput. Fluids 124 (2016) 185–189.
[213] M.K. Borg, D.A. Lockerby, J.M. Reese, Fluid simulations with atomistic resolution: a hybrid multiscale method with field-wise coupling, J. Comput. Phys. 255 (2013) 149–165.
[214] M.K. Borg, D.A. Lockerby, J.M. Reese, A hybrid molecular-continuum simulation method for incompressible flows in micro/nanofluidic networks, Microfluid. Nanofluid. 15 (4) (2013) 541–557.
[215] M.K. Borg, D.A. Lockerby, J.M. Reese, A hybrid molecular–continuum method for unsteady compressible multiscale flows, J. Fluid Mech. 768 (2015) 388–414.
[216] A. Patronis, D.A. Lockerby, M.K. Borg, J.M. Reese, Hybrid continuum–molecular modelling of multiscale internal gas flows, J. Comput. Phys. 255 (2013) 558–571.
[217] K. Ritos, M.K. Borg, D.A. Lockerby, D.R. Emerson, J.M. Reese, Hybrid molecular-continuum simulations of water flow through carbon nanotube membranes of realistic thickness, Microfluid. Nanofluid. 19 (5) (2015) 997–1010.
[218] M.K. Borg, J.M. Reese, Multiscale simulation of enhanced water flow in nanotubes, MRS Bull. 42 (4) (2017) 294–299.
[219] X. Yue, W. E, The local microscale problem in the multiscale modeling of strongly heterogeneous media: effects of boundary conditions and cell size, J. Comput. Phys. 222 (2) (2007) 556–572.
[220] E.J. Carr, I.W. Turner, P. Perre, A dual-scale modeling approach for drying hygroscopic porous media, Multiscale Model. Simul. 11 (1) (2013) 362–384.
[221] E.J. Carr, P. Perré, I.W. Turner, The extended distributed microstructure model for gradient-driven transport: a two-scale model for bypassing effective parameters, J. Comput. Phys. 327 (2016) 810–829.
[222] E. Lorenz, A.G. Hoekstra, Heterogeneous multiscale simulations of suspension flow, Multiscale Model. Simul. 9 (4) (2011) 1301–1326.
[223] C.W. Gear, J. Li, I.G. Kevrekidis, The gap-tooth method in particle simulations, Phys. Lett. A 316 (3–4) (2003) 190–195.
[224] C. Theodoropoulos, K. Sankaranarayanan, S. Sundaresan, I.G. Kevrekidis, Coarse bifurcation studies of bubble flow lattice Boltzmann simulations, Chem. Eng. Sci. 59 (12) (2004) 2357–2362.
[225] P. Van Leemput, K.W.A. Lust, I.G. Kevrekidis, Coarse-grained numerical bifurcation analysis of lattice Boltzmann models, Physica D 210 (1–2) (2005) 58–76.
[226] M.E. Kavousanakis, C.E. Colosqui, I.G. Kevrekidis, A.G. Papathanasiou, Mechanisms of wetting transitions on patterned surfaces: continuum and mesoscopic analysis, Soft Matter 8 (30) (2012) 7928–7936.
[227] C. Vandekerckhove, P. Van Leemput, D. Roose, Acceleration of lattice Boltzmann models through state extrapolation: a reaction–diffusion example, Appl. Numer. Math. 58 (11) (2008) 1742–1757.
[228] C. Yang, H. He, Simulation of liquid–vapour phase transitions and multiphase flows by an improved lattice Boltzmann model, Int. J. Comput. Fluid Dynam. 29 (9–10) (2015) 423–433.
[229] S. Sirisup, G.E. Karniadakis, D. Xiu, I.G. Kevrekidis, Equation-free/Galerkin-free POD-assisted computation of incompressible flows, J. Comput. Phys. 207 (2) (2005) 568–587.
[230] V. Esfahanian, K. Ashrafi, Equation-Free/Galerkin-Free reduced-order modeling of the shallow water equations based on proper orthogonal decomposition, J. Fluids Eng. 131 (7) (2009) 071401.
[231] S.J. Moon, S. Sundaresan, I.G. Kevrekidis, Coarse-grained computations of demixing in dense gas-fluidized beds, Phys. Rev. E 75 (5) (2007) 051309.
[232] J. Liu, S.Y. Chen, X.B. Nie, M.O. Robbins, A continuum-atomistic multi-timescale algorithm for micro/nano flows, Comm. Comput. Phys. 4 (5) (2008) 1279–1291.
[233] M.G. Pérez, E. Vakkilainen, T. Hyppänen, 2D dynamic mesh model for deposit shape prediction in boiler banks of recovery boilers with different tube spacing arrangements, Fuel 158 (2015) 139–151.
[234] Z. Guo, B. Shi, C. Zheng, A coupled lattice BGK model for the Boussinesq equations, Int. J. Numer. Meth. Fluids 39 (4) (2002) 325–342.
[235] Z. Guo, T.S. Zhao, Lattice Boltzmann model for incompressible flows through porous media, Phys. Rev. E 66 (3) (2002) 036304.
[236] F.F. Abraham, J.Q. Broughton, N. Bernstein, E. Kaxiras, Spanning the continuum to quantum length scales in a dynamic simulation of brittle fracture, Europhys. Lett. 44 (6) (1998) 783.
[237] S.C.L. Kamerlin, S. Vicatos, A. Dryga, A. Warshel, Coarse-grained (multiscale) simulations in studies of biophysical and chemical systems, Annu. Rev. Phys. Chem. 62 (2011) 41–64.
[238] V.H. Vu, B. Trouette, Q.D. To, E. Chénier, Multi-scale modelling and hybrid atomistic-continuum simulation of non-isothermal flows in microchannels, Microfluid. Nanofluid. 20 (2) (2016) 43.
[239] B. Rouet-Leduc, K. Barros, E. Cieren, V. Elango, C. Junghans, T. Lookman, J. Mohd-Yusof, R.S. Pavel, A.Y. Rivera, D. Roehm, A.L. McPherson, T.C. Germann, Spatial adaptive sampling in multiscale simulation, Comput. Phys. Commun. 185 (7) (2014) 1857–1864.

[240] Q. Nie, Y. Joshi, Multiscale thermal modeling methodology for thermoelectrically cooled electronic cabinets, Numer. Heat Transfer, Part A: Appl. 53 (3) (2007) 225–248.
[241] E. Samadiani, Y. Joshi, Multi-parameter model reduction in multi-scale convective systems, Int. J. Heat Mass Transf. 53 (9–10) (2010) 2193–2205.
[242] Y. Joshi, Reduced order thermal models of multiscale microsystems, J. Heat Transfer 134 (3) (2012) 031008.
[243] F. Sarghini, G. De Felice, S. Santini, Neural networks based subgrid scale modeling in large eddy simulations, Comput. Fluids 32 (1) (2003) 97–108.
[244] M. Ma, J. Lu, G. Tryggvason, Using statistical learning to close two-fluid multiphase flow equations for a simple bubbly system, Phys. Fluids 27 (9) (2015) 092101.
[245] M. Ma, J. Lu, G. Tryggvason, Using statistical learning to close two-fluid multiphase flow equations for bubbly flows in vertical channels, Int. J. Multiph. Flow 85 (2016) 336–347.
[246] N. Asproulis, D. Drikakis, An artificial neural network-based multiscale method for hybrid atomistic-continuum simulations, Microfluid. Nanofluid. 15 (4) (2013) 559–574.
[247] D. Stephenson, J.R. Kermode, D.A. Lockerby, Accelerating a hybrid continuum-atomistic fluidic model with on-the-fly machine learning. arXiv preprint arXiv:1603.04628, 2016.
[248] D. Roehm, R.S. Pavel, K. Barros, B. Rouet-Leduc, A.L. McPherson, T.C. Germann, C. Junghans, Distributed database kriging for adaptive sampling (D^2KAS), Comput. Phys. Commun. 192 (2015) 138–147.